Dimitrios G. Pavlou

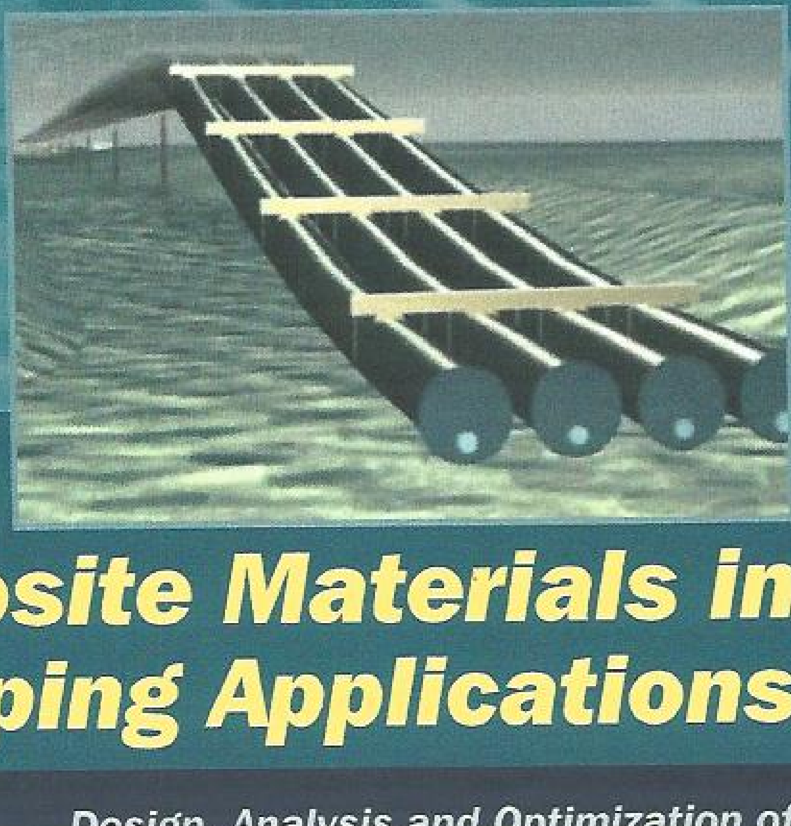

Composite Materials in Piping Applications

Design, Analysis and Optimization of Subsea and Onshore Pipelines from FRP Materials

Composite Materials in Piping Applications

DEStech Publications, Inc.
439 North Duke Street
Lancaster, Pennsylvania 17602 U.S.A.

Printed in the United States of America
10 9 8 7 6 5 4 3 2 1

Main entry under title:

Composite Materials in Piping Applications: Design, Analysis and Optimization of Subsea and Onshore Pipelines from FRP Materials

A DEStech Publications book
Bibliography: p.
Includes index p. 395

Library of Congress Control Number: 2013935448
ISBN No. 978-1-60595-029-7

CHAPTER 6

Creep Design of Piping Applications Using Composite Materials

RUI MIRANDA GUEDES[1] AND HUGO FARIA[2]

[1]Department of Mechanical Engineering (DEMec), Faculty of Engineering of the University of Porto (FEUP), Rua Dr. Roberto Frias s/n, 4200-465 Porto, Portugal.

[2]INEGI-Instituto de Engenharia Mecânica e Gestão Industrial, Rua Dr. Roberto Frias, 400, 4200-465 Porto, Portugal

6.1 INTRODUCTION

The application of glass fiber-reinforced thermoset matrix composites as primary structures has been impeded by a number of problems. Ochoa and Salama [1] pointed out five basic reasons, which include two very difficult challenges: the need to have databases for long-term damage mechanisms for lifetime prediction and the need for nondestructive evaluation (NDE) and in-service monitoring. Both are interrelated in terms of simulating service loads, manufacturing, and installation procedures. The proper environmental and loading conditions used to accelerate long-term testing are not fully known in advance. To be representative, they must generate damage evolution and failure modes similar those occurring in real conditions over 20 to 30 years. The heterogeneity and anisotropy introduced by the fiber and matrix make such an analysis very complicated. Moreover any change in the manufacturing procedure, matrix or fiber, produces a different material system, which in turn invalidates the use of previous experimental databases.

Pipelines, risers and piping systems are examples of primary applications of filament-wound composites in the oil and gas industry. The thermosetting resins commonly used are epoxy and polyester resin systems. The advantages are well known: high stiffness-to-weight ratio and corrosion resistance.

The design of these structures is highly demanding, since they are expected to remain in service for more than 20 years. During service, pipe structures may be subjected to both permanent and cycling loads. Although they do offer high mechanical performance, over time their strength and stiffness may decay significantly, a consequence of the viscoelastic nature of the matrix, damage accumulation within the matrix and fiber breakage. One serious consequence of these events is premature failure, usually catastrophic.

The lack of full understanding of the fundamental parameters controlling long-term materials' performance necessarily leads to over-design. In this context, the lifetime prediction of these structures is an important issue not completely solved. Standards for certification of glass reinforced plastic (GRP) pipes require at least 10,000 hours of testing and a high number of specimens. Even though these stringent requirements may be seen as reasonable in terms of safety, they severely restrict the improvement and innovation of new products, which in turn may inhibit greater commercial penetration in the markets.

The present chapter will present the following argument. The second section reviews selected theoretical approaches for long-term failure criteria. Time-dependent failure criteria are presented and developed in a manner useful for practical engineering applications. The third section attempts to couple damage with creep and fatigue effects on a long-term basis, based on safety factors. It starts with a brief theoretical description of damage initiation and propagation during static loading. Long-term sustained and cycling loads usually produce damage similar to that originated under quasi-static loading. Experimental creep failure data under sustained hydrostatic pressure are presented, followed by an example of preliminary design for long-term creep. The fourth section is devoted to fatigue failure. Experimental data published for filament-wound pipe failure under cycling hydrostatic pressure are presented and discussed. The fifth section describes and compares the standards for the design and qualification of pipes. Finally, the sixth section presents a worked example with preliminary calculations of qualification pressure for a filament-wound pipe, using known material properties, based on ISO 14692.

6.2 CREEP DAMAGE ACCUMULATION MECHANISMS IN COMPOSITE MATERIALS

In engineering, creep designates the gradual increase in strain that occurs in a material when it is subjected to a sustained load over a certain period of time. Even at room temperature polymers and polymer-based composites can undergo creep at relatively low stress levels. Moreover, given enough time, creep will lead to rupture.

Usually the creep strain evolution may be divided into three distinct regions: I) first-stage or primary creep, which starts at a rapid rate and slows with time; II) second-stage (secondary) creep, where creep has a relatively uniform rate (minimum gradient); III) third-stage (tertiary), where creep manifests an accelerating creep rate and terminates with failure of the material. This is illustrated schematically in Figure 6.1.

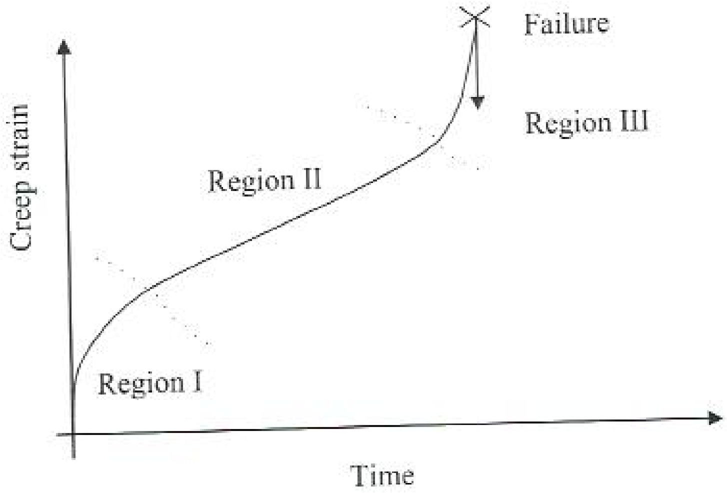

Figure 6.1 Typical creep strain evolution divided into three regions.

General strength theories do not include the creep-to-yield or creep-to-rupture process. Since the stress-strain analysis is based on continuum mechanics, a difficulty presents itself when attempts are made to predict failure in general and creep failure in particular of polymers and polymer matrix based composites. Fracture mechanics and damage mechanics include the distribution of defects into continuum models, which allow time-dependent failure prediction. Energy-based failure criteria provide another possible approach. An example is establishing that the energy accumulated in the springs of the viscoelastic mechanical model, designated as free energy, has a limit value. This limit can be or not be constant. Earlier approaches to the prediction of time-dependent failures provided explicit elementary equations to predict behavior over a lifetime. Following this line, a global and homogeneous analysis was chosen because it is more convenient for practical engineering applications.

In this context it becomes important to predict the effects of long-term loading on deformation and failure behavior. A reliable prediction requires the use of models that capture accurately the stress/strain time-dependent evolution of the filament-wound cylindrical pipes. Most plastics, composites and other synthetic materials exhibit strong hereditary type non-linear viscoelastic behaviors, which render any stress-strain analysis of these materials a significant challenge. Single-integral formulations, such as the Schapery nonlinear viscoelastic theory [2], have proven to be very effective in representing the creep strain of filament-wound pipes [3]:

$$\varepsilon(t) = J_0 g_0 \sigma(t) + g_1 \int_0^t \Delta J(\psi - \psi') \frac{d(g_2 \sigma(\tau))}{d\tau} d\tau \tag{6.1}$$

with the correspondent reduced times Ψ and Ψ' given by:

$$\Psi = \int_0^t \frac{d\tau'}{a_\sigma} \quad , \quad \Psi' = \int_0^\tau \frac{d\tau'}{a_\sigma} \tag{6.2}$$

where g_0, g_1, g_2, a_σ are stress-dependent nonlinearizing parameters. The kernel $\Delta J(t)$ is the time-dependent compliance. The compliance is usually expressed by a power law [2–4]:

$$\Delta J(t) = J_1 t^n \tag{6.3}$$

where J_1, n are linear viscoelastic parameters.

Ghorbel [3] simplified the Schapery formulation since he did not perform all the necessary creep and creep-recovery tests to obtain the full material stress-dependent nonlinearizing parameters. Furthermore, it was found that $g_0 = 1$. The simplified expression for strain creep under sustained load was

$$\varepsilon(t) = \varepsilon(0) + g(\sigma)t^n \tag{6.4}$$

where $g(\sigma) = \beta\sigma^m$ and β and m are material properties.

It must be emphasized that long-term strain creep measurement for filament-wound cylinders is not usually done; only the time-to-failure is needed to qualify pipes.

In the case of multi-directional filament-wound pipes, it is possible to perform elastic-viscoelastic analyses using an approach based on classical laminated plate theory (CLPT) as exemplified in [5]. That specific methodology includes a time-dependent failure criterion. However for thick cylinders the CLPT approach does not work. Hence a method to calculate the time-dependent stress-strain state in nonlinear viscoelastic thick multilayered composite cylinders was proposed and implemented [6]. This work demonstrated the importance of the viscoelasticity effect over the time-dependent internal stress distribution through thick laminated cylinders.

One of the first theoretical attempts to include time in a material strength formulation for viscoelastic materials was developed by Reiner and Weissenberg [7]. The Reiner-Weissenberg criterion [7] states that the work done during the loading by external forces on a viscoelastic material is converted into a stored portion (potential energy) and a dissipated portion (loss energy). Hence the criterion assumes that the instant of failure depends on a conjunction between distortional free energy and dissipated energy, with the threshold value of the distortional energy being the governing quantity.

Let us assume that the unidirectional strain response of a linear viscoelastic material under arbitrary stress $s(t)$, is given by the power law as:

$$\varepsilon(t) = D_0\sigma(t) + D_1\int_0^t \left(\frac{t-\tau}{\tau_0}\right)^n \frac{\partial\sigma(\tau)}{\partial\tau} d\tau \tag{6.5}$$

where D_0, D_1, n are material constants and t_0 represents the time unity (equal to 1 second or 1 hour or 1 day, etc.).

The free stored energy, using the Hunter [8] formulation, is given by:

$$W_s(t) = \varepsilon(t)\sigma(t) - \frac{1}{2}D_0\sigma(t)^2 - \frac{1}{2}\int_0^t\int_0^t D_1\left(\frac{2t-\tau_1-\tau_2}{\tau_0}\right)^n \frac{\partial\sigma(\tau_1)}{\partial\tau_1}\frac{\partial\sigma(\tau_2)}{\partial\tau_2} d\tau_1 d\tau_2 \tag{6.6}$$

The total energy is defined as:

$$W_t(t) = \int_0^t \sigma(\tau)\frac{\partial\varepsilon(\tau)}{\partial\tau} d\tau\ . \tag{6.7}$$

Accordingly, these time-dependent failure criteria [9] predict the lifetime under constant load as a function of the applied load s_0 and the strength under an instantaneous condition s_R:

The Reiner-Weissenberg Criterion (R-W) states that $W_s(t) \le \frac{D_0}{2}\sigma_R^{\ 2}$,

$$\left(\frac{t_f}{\tau_0}\right) = \left(\frac{1}{2-2^n}\right)^{\frac{1}{n}} \left(\frac{D_0}{D_1}\right)^{\frac{1}{n}} \left(\frac{1}{\gamma}-1\right)^{\frac{1}{n}}. \tag{6.8}$$

The Maximum Work Stress Criterion (MWS) states that $W_t(t) \le \frac{D_0}{2}\sigma_R^{\ 2}$,

$$\left(\frac{t_f}{\tau_0}\right) = \left(\frac{1}{2}\frac{D_0}{D_1}\right)^{\frac{1}{n}} \left(\frac{1}{\gamma}-1\right)^{\frac{1}{n}}. \tag{6.9}$$

The Maximum Strain Criterion (MS) states that $\varepsilon(t) \le D_0\sigma_R$,

$$\left(\frac{t_f}{\tau_0}\right) = \left(\frac{D_0}{D_1}\right)^{\frac{1}{n}} \left(\frac{1}{\sqrt{\gamma}}-1\right)^{\frac{1}{n}}. \tag{6.10}$$

The modified Reiner-Weissenberg Criterion (MR-W) states that

$$W_t(t) \le \left(\frac{D_0}{2}\sigma_R\right)\sigma(t),$$

$$\left(\frac{t_f}{\tau_0}\right) = \left(\frac{1}{2-2^n}\right)^{\frac{1}{n}} \left(\frac{D_0}{D_1}\right)^{\frac{1}{n}} \left(\frac{1}{\sqrt{\gamma}}-1\right)^{\frac{1}{n}}. \tag{6.11}$$

where $\gamma = \sigma_0^{\,2}/\sigma_R^{\,2}$.

In short, these approaches establish a relationship between time to failure, viscoelastic properties and static stress failure throughout a stored elastic energy limit concept. As an approximation, it is not difficult to conclude that we can take $t\sim\sigma^{-2/n}$ for the R–W and the MSW criteria and $t\sim\sigma^{-1/n}$ for the MS and the MR-W criteria. Similar results were obtained using fracture mechanics concepts [10]. In fact, these concepts established a relationship between time-to-failure, viscoelastic properties and strength properties [11-12], which are similar to the previous approach. The main difference in these failure criteria is the interpretation of the physical constants. According to Song et al. [13], there are three major phenomena, which frequently occur simultaneously, responsible for the creep failure of viscoelastic materials: (1) time-dependent constitutive equations; (2) time to the formation of overstressed polymer chains in a localized plastic area, i.e., a fracture initiation mechanism; and (3) the kinetics of molecular flow and bond rupture of the overstressed polymer chains. The fracture mechanics approach assumes the existence of defects from the start and develops a theory about the kinetic crack growth, i.e., the fracture initiation process is neglected. In the previous approach, the stored energy in the material, i.e., the energy stored by all springs in the viscoelastic model, can be compared with the energy necessary to stretch the polymer chains and promote their bond rupture. In fact, it is possible to visualize the polymer chains as linear springs acting as energy accumulators. Nevertheless, these energy accumulators have a limited capacity above which bond rupture occurs. Therefore the stored energy limit, called *critical energy*, can be related to the energy involved in all microscale bond ruptures that lead to creep-rupture. Most probably this critical energy depends on the internal state. In reality, there are experimental indications that the critical energy is temperature- and strain-rate- dependent [14], at least for temperatures lower than the glass transition temperature Tg (or for shorter times). This means that the R–W criterion is not universal. On the other hand, there is experimental evidence, for polymers and composite polymers, that change in the fracture mode is a result of change in critical energy with temperature and strain rate [14]. Finally, it is not difficult to accept that creep-rupture is strongly related to creep compliance or relaxation modulus. This relationship emerges naturally from theoretical approaches like fracture mechanics and energy criteria. Furthermore, creep-rupture and relaxation modulus variations over time, measured experimentally, resemble one another in an extraordinary manner. Most probably this signifies that a change in the relaxation modulus corresponds to a change in the strength.

The rate theory of fracture is based on a molecular approach, i.e., on the kinetics of molecular flow and the bond rupture of the polymer chains. Drawing on these approaches Zhurkov [15] presented one of the first models for predicting a material's lifetime t_f (except for very small stresses) in terms of a constant stress level σ,

$$t_f = t_0 \exp\left[\left(U_0 - \gamma\sigma\right)/kT\right], \tag{6.12}$$

where t_0 is a constant on the order of the molecular oscillation period of 10^{-13}s, k is the Boltzmann constant, T is the absolute temperature, U_0 is a constant for each material regardless its structure and treatment, and γ depends on the previous treatments of the material and varies over a wide range for different materials. Griffith et al. [16] applied a modified version of the Zurkov equation:

$$t_f = t_0 \exp\left(\frac{U_0}{kT} - \gamma\sigma\right), \tag{6.13}$$

known as the modified rate equation, for predicting the time to rupture of continuous fiber-reinforced plastics with reasonable success.

The fracture mechanics analysis was extended to viscoelastic media to predict the time-dependent growth of flaws or cracks. Several authors produced extensive work in this area [11,12,17–20]. Schapery [19,20] developed a theory of crack growth that was used to predict the crack speed and lifetime for an elastomer under uniaxial and biaxial stress states. For a centrally cracked viscoelastic plate with a creep compliance given by eq. (6.5) under constant load, Schapery [11] deduced, after some simplifications, a simple relationship between stress and time to failure:

$$\left(\frac{t_f}{\tau_0}\right) = \left(B\sigma_0\right)^{-2(1+1/n)}, \tag{6.14}$$

where n is the exponent of the creep compliance power law and B a parameter that depends on the geometry and properties of the material. Leon and Weitsman [21] and Corum et al. [22] used this approach where B was considered an experimental constant, to fit creep-rupture data with considerable success. Christensen [23] developed a kinetic crack formulation to predict the creep rupture lifetime for polymers. The lifetime was determined from the time required for an initial crack to grow sufficiently large to cause failure. The method assumed quasi-static conditions and applies only to the central crack problem. The polymeric material was taken to be in the glassy elastic state, as would be normal in most applications. For general stress, $\sigma(t)$ we have:

$$1-\left(\sigma(t)/\sigma_R\right)^{1/m}=\int_0^{t_f/(\alpha\tau_0)}\left(\sigma(\tau)/\sigma_R\right)^{1/m+1}d\tau, \tag{6.15}$$

where $\gamma=\sigma_0^{\,2}/\sigma_R^{\,2}$, m is the exponent of the power law relaxation function and α is a parameter governed by the geometry and viscoelastic properties. For constant stress, $\sigma=\sigma_0$, the lifetime is given as:

$$\left(\frac{t_f}{\tau_0}\right)=\frac{\alpha}{\sqrt{\gamma}}\left(\frac{1}{\sqrt{\gamma}^{\,1/m}}-1\right). \tag{6.16}$$

A classical approach for considering the degradation of mechanical properties is provided by the method of continuum damage mechanics (CDM). Following the original ideas of Kachanov [24], the net stress, defined as the remaining load-bearing cross-section of the material is given [25] by:

$$\tilde{\sigma}=\frac{\sigma}{1-\omega}, \tag{6.17}$$

where $0\le\omega\le1$ is the damage variable. At rupture, no load-bearing area remains, and the net stress tends to infinity when $\omega\to1$.

Kachanov [24] assumes the following damage growth law:

$$\dot{\omega}(t)=C\left(\frac{\sigma(t)}{1-\omega(t)}\right)^{v}, \tag{6.18}$$

where C and v are material constants. This equation leads to a separable differential equation for $\omega(t)$, assuming $\omega(0)=0$

$$\left(1-\omega(t)\right)^{v}\dot{\omega}(t)=C\sigma^{v}(t)\Rightarrow1-\left(1-\omega(t)\right)^{1+v}=C(1+v)\int_0^t\sigma^{v}(\tau)\,d\tau. \tag{6.19}$$

The damage growth law is given as:

$$\omega(t)=1-\left[1-C(1+v)\int_0^t\sigma^{v}(\tau)\,d\tau\right]^{\frac{1}{1+v}}. \tag{6.20}$$

Assuming failure when $\omega = 1$, then the following expression is obtained:

$$C(1+\nu)\int_0^t \sigma^\nu(\tau)\,d\tau = 1. \tag{6.21}$$

From the previous relationship, the time to failure for creep is readily obtained, assuming $\sigma(t) = \sigma_0$,

$$t_c = \frac{1}{C(1+\nu)\sigma_0^\nu}. \tag{6.22}$$

Clearly, this result is equivalent to the one obtained previously by using the Schapery theory [11]. Therefore, the creep lifetime expressions obtained for both theoretical approaches are directly comparable and are, in fact, equivalent, even though the parameters have distinct physical interpretations.

Damage evolution does depend strongly on a number of different factors acting simultaneously, i.e., temperature, moisture, stress, viscoelasticity, viscoplasticity, etc. Each of these factors is time-dependent. In practice, the influence of any one on long-term failure is measured independently, i.e., under constant conditions. Hence, a further methodology is needed to account for their combined effects.

One crucial question remaining to be solved completely is how to predict damage accumulation, or the remaining strength, after a fatigue or creep cycle at multiple stress levels, based on the fatigue and creep master curves. Miner's Rule [26] is an example of a simple way to account for damage accumulation due to different fatigue cycles. This damage fraction rule is also designated as the Linear Cumulative Damage law (LCD). For fatigue, it states that failure occurs when the following condition is satisfied:

$$\sum_i^N \frac{\Delta n_i(\sigma_i)}{n_f(\sigma_i)} = 1, \tag{6.23}$$

where n_f is the number of cycles to failure at stress level σ_i and Δn_i is the number of cycles applied at each stress level σ_i of the fatigue cycle. Hence eq. (6.23) provides a failure criterion for fatigue. The corresponding form for creep conditions is given by:

$$\sum_i^N \frac{\Delta t_i(\sigma_i)}{t_c(\sigma_i)} = 1, \tag{6.24}$$

where t_c is the creep rupture lifetime at stress level σ_i and Δt_i is the time applied at each stress level σ_i. Once more, equations (6.23) and (6.24) specify a criterion for a lifetime at multiple stress levels. Later, Bowman and Barker [27] suggested a combination of both damage fraction rules to analyze experimental data for thermoplastics tested until failure under a trapezoidal loading profile, which combined fatigue with creep. Although the Miner's rule can predict accurately the failure of fiber-reinforced polymers under certain combined stress levels, it proved to be inadequate in many other cases. However, due to its simplicity, it is still used in engineering design.

A cumulative damage theory developed to address various applied problems in which time, temperature, and cyclic loading are given explicitly, was developed by Reifsnider et al. [28–30].

The basic form of the strength evolution equation calculates the remaining strength F_r

$$F_r = 1 - \int_0^z \left(1 - F_a\left(\frac{\sigma(\tau)}{X(\tau)}\right)\right) j\tau^{j-1} d\tau , \tag{6.25}$$

where $z = t/\tau$, t is the time variable, τ is a characteristic time associated with the process, F_a is the normalized failure function that applies to a specific controlling failure mode, and j is a material parameter. This material parameter does influence damage progression. If $j < 1$, the rate of degradation is greatest at the beginning, but if $j > 1$, the rate of degradation increases as a function of time. However, if $j = 1$, there is no explicit time dependence in the rate of degradation. The failure criterion is given by $F_r = F_a$. This approach has been used successfully for more than 20 years by Reifsnider et al. [28–30] to solve various applied problems where time, temperature, and cyclic loading are explicit influences.

6.3 SHORT AND LONG-TERM STATIC FAILURE OF COMPOSITE PIPES

6.3.1 Damage modeling

The application of damage mechanics enables one to model the matrix degradation resulting from cracking in filament-wound pipes [31]. This damage is quantified in terms of crack density, i.e., the reciprocal of crack spacing. The model used by Roberts et al. [32], based on the previous work of Zang and Gudmundson [33], applies to microcracks with crack surfaces parallel to the fiber direction and perpendicular to the lamina plane. In the end, the stiffness matrix of each ply is obtained by subtracting the damage tensor from the ply stiffness as:

$$Q_{ij}^{total} = Q_{ij}^{elastic} - Q_{ij}^{damage} , \tag{6.26}$$

where
$$Q_{ij}^{elastic} = \begin{bmatrix} \dfrac{E_1}{1-\nu_{12}\nu_{21}} & \nu_{12}\dfrac{E_2}{1-\nu_{12}\nu_{21}} & 0 \\ & \dfrac{E_2}{1-\nu_{12}\nu_{21}} & 0 \\ Sym. & & G_{12} \end{bmatrix}$$

and
$$Q_{ij}^{damage} = \rho \begin{bmatrix} \beta_2\left(\nu_{12}\dfrac{E_1}{1-\nu_{12}\nu_{21}}\right)^2 & \beta_2\left(\nu_{12}\dfrac{E_1}{1-\nu_{12}\nu_{21}}\right)\left(\dfrac{E_2}{1-\nu_{12}\nu_{21}}\right) & 0 \\ & \beta_2\left(\dfrac{E_2}{1-\nu_{12}\nu_{21}}\right)^2 & 0 \\ Sym. & & \beta_1 G_{12}^2 \end{bmatrix}$$

where E_1 is the longitudinal modulus (in the fiber direction), E_2 is the transverse modulus (perpendicular to the fiber direction), ν_{12} is the major in-plane Poisson's ratio (i.e., the Poisson's ratio that corresponds to a contraction in the transverse direction when an extension is applied in the longitudinal direction and is related to the minor in-plane Poisson's ratio by $\nu_{21}/E_2 = \nu_{12}/E_1$), and G_{12} is the in-plane shear modulus. The dimensionless or normalized crack density in the ply is defined by the ratio of ply thickness and crack spacing $\rho = t/s$. The coefficient β_1 relates to crack-face displacement in Mode III anti-plane strain, and the coefficient β_2 relates to a Mode I crack opening. These two coefficients are expressed by:

$$\begin{aligned} \beta_1 &= \frac{2}{\pi G_{12}\rho^2}\ln\cosh\left(\frac{\pi}{2}\rho\right) \\ \beta_2 &= \frac{\pi}{2}\left(\frac{1-\nu_{12}\nu_{21}}{E_2}\right)\sum_{n=1}^{10}\frac{a_n}{(1+\rho)^n} \end{aligned}, \tag{6.27}$$

where the constants a_n are tabulated in [32]. For a ply with a free surface, β_1 is 2.0 times, and β_2 2.51 times, their corresponding values [34].

The crack density effect on elastic constants is shown in Figure 6.2, with the results normalized by its initial undamaged value, which is obtained from classical laminated plate theory (CLPT) coupled with equation (22.6). The main conclusion for angle-ply laminates is that the axial modulus decreases most rapidly with increasing crack density. Frost [31] suggested an approximation using a linear

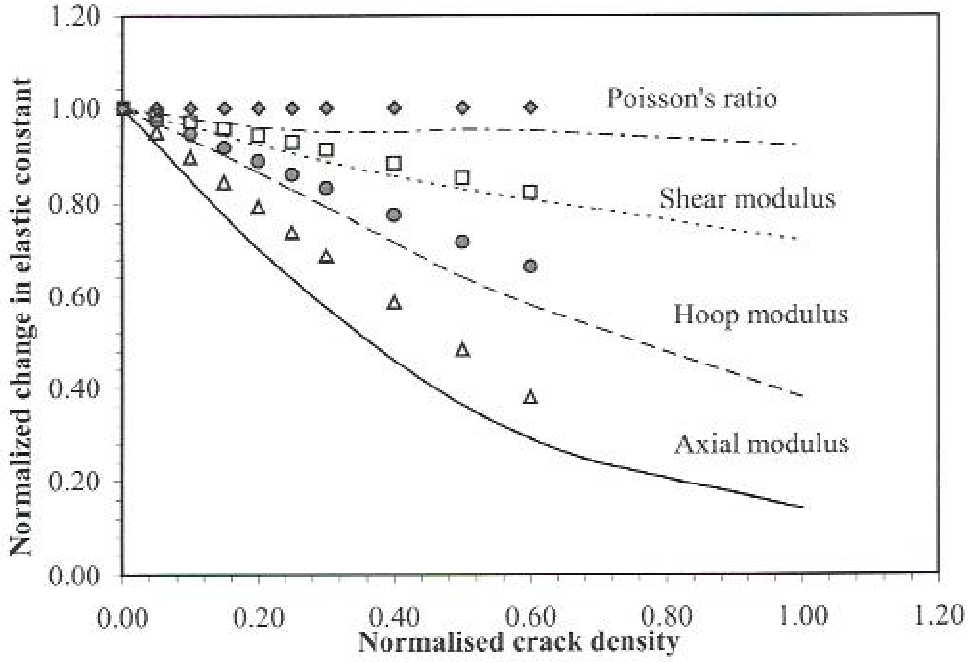

Figure 6.2 Normalized change in elastic constants versus crack density for ±55° pipe laminate, calculated from the model of Roberts at al. [32] (lines) and using the linear approximation given by Frost [31] (points).

relationship for elastic properties that decay with crack normalized density. The simplified approach proposed by Frost [31] captures the initial changes in elastic properties, as depicted in Figure 6.2. The observed differences arise from the fact that the elastic material properties are not exactly the same. Hence, this simplified approach does predict relevant decay in the pipe's elastic properties with good accuracy for the important crack density range prior to failure.

The relation between the crack density and the applied stress, for each ply, was approximated as:

$$1+k^2\rho^2=\sqrt{f(\sigma_2,\tau_{12})}\ [31], \tag{6.28}$$

with
$$k^2=\frac{(E_1+E_2)G_{12}}{E_1E_2}$$

and
$$f(\sigma_2,\tau_{12})=\left(\frac{\sigma_2}{\sigma_{2,failure}}\right)^2+\left(\frac{\tau_{12}}{\tau_{12,failure}}\right)^2-\frac{\sigma_2}{\sigma_{2,failure}}\frac{\tau_{12}}{\tau_{12,failure}}$$

where σ_2 and τ_{12} represent the ply transverse and shear stresses and $\sigma_{2,failure}$, and $\tau_{12,failure}$ the respective failure stresses. The function in (6.24) gives the normalized crack density as a function of a second-order polynomial that depends on both the shear and transverse stresses, which are the stresses contributing to crack formation. Since the stiffness in (6.22) depends on crack density, a nonlinear stress–strain relation is obtained. This was applied by Roberts et al. [32] to the deformation of internally pressurized pipes with promising results.

The methodology is easy to implement, and some calculations were performed using data for E-glass/epoxy ±55° filament-wound pipes provided by Soden et al. [35–36]. In Figures 6.3 and 6.4, predictions and experimental data are compared for stress-strain response under two different modes: hydrostatic pressure with closed and open ends. The theory provides a good approximation to the stress-strain experimental curves.

In general, the failure parameter is given as:

$$f(\sigma_2, \tau_{12}) = C, \tag{6.29}$$

For short-term and non-aged samples, $C = 1$. In cases of long-term analysis, the failure parameter becomes dependent on time, static or cyclic loading and temperature:

$$C = A_{creep} A_{Temperature} A_{fatigue}, \tag{6.30}$$

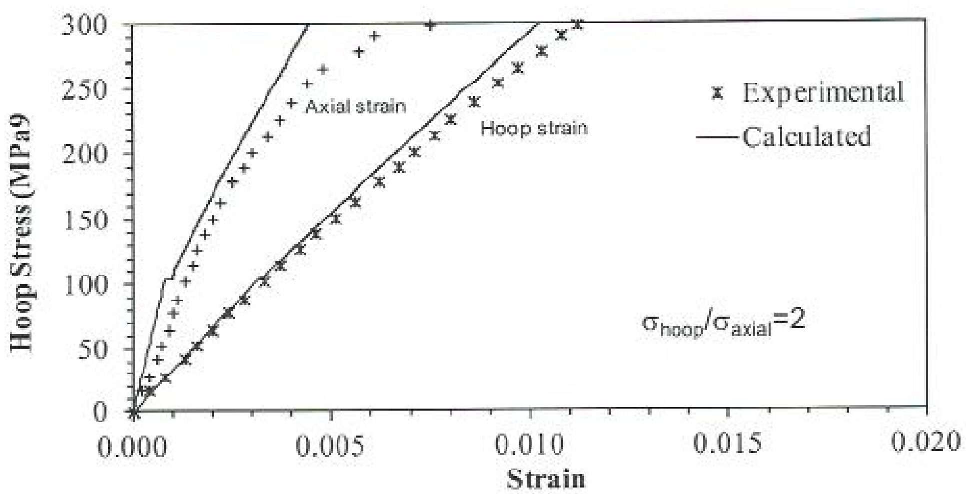

Figure 6.3 Comparison between experimental data and predictions of the stress-strain behavior of an E-glass/epoxy ±55° filament-wound pipe under hydrostatic pressure with closed ends.

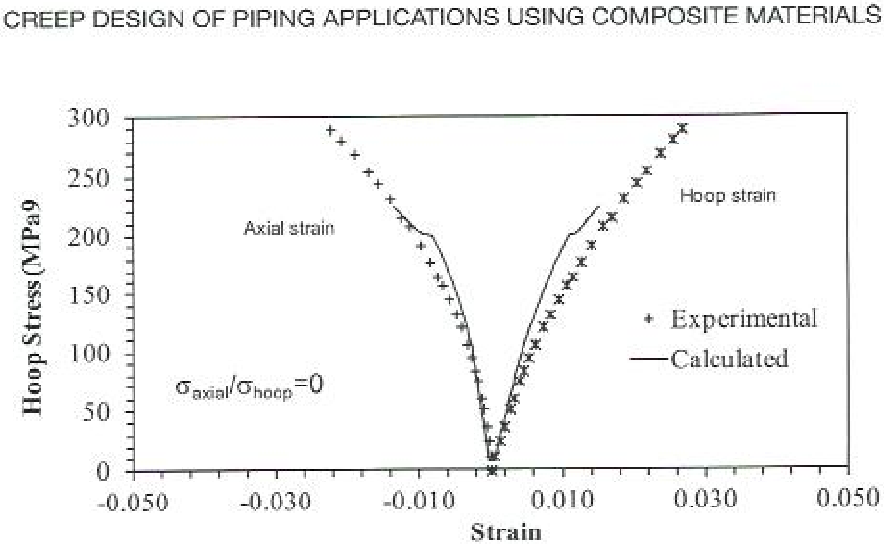

Figure 6.4 Comparison between experimental data and predictions of the stress-strain behavior of an E-glass/epoxy ±55° filament-wound pipe under hydrostatic pressure with open ends.

According to Frost [31], for long-term sustained loading the factor A_{creep} can be set to 0.5 for 20-year conservative design. Using this assumption and the previous theoretical approach, it is possible to predict the failure envelope for short-term and long-term cases under different loading modes, as shown in Figure 6.5, for an E-glass/epoxy ±55° filament-wound pipe. Failure was assumed to occur when the normalized crack density reaches the value of 0.5 (2.2mm for a ply thickness of 0.25mm).

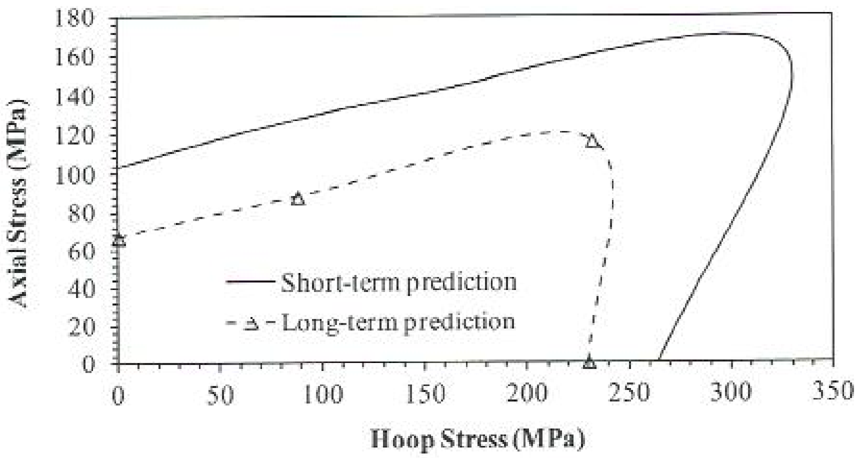

Figure 6.5 Predicted failure envelope for short-term and long-term sustained loadings on an E-glass/epoxy ±55° filament-wound pipe.

In general, the failure mechanism of most glass-reinforced plastics, like filament-wound pipes, does not change from short to long term. Based on this assumption and using the Paris law, Frost [31] showed that the creep factor may be given as:

$$A_{creep} = \frac{1}{t^{\alpha}}, \tag{6.30}$$

where α is equal to the time exponent obtained by regression of the creep failure curves.

For cyclic loads exceeding 7000 cycles over the design life, fatigue effects must be considered. These effects are more severe than creep effects. The standard ISO 14692-3:2002 proposes the following factor:

$$A_{fatigue} = \sqrt{\left(R^2 + \frac{1}{16}\left(1 - R^2\right)\right)} \exp\left[\left(1 - R^2\right)\left(1 - \frac{N - 7000}{10^8}\right)\right], \tag{6.32}$$

where R is the ratio between the minimum and maximum loads (or stresses) of the load (or stress) cycle and N is the total number of cycles during service life.

For illustration purposes an example of static (creep) and cyclic pipe test results at 65°C can be cited from [37]. In Figure 6.6, the creep failures curves are shown, and in Figure 6.7 the experimental data and the predicted curves are represented. The fatigue curves were predicted from creep failure curves using the factor $A_{fatigue}$ from ISO 14692-3:2002, with $R = 0$. The predictions are very close to experimental data.

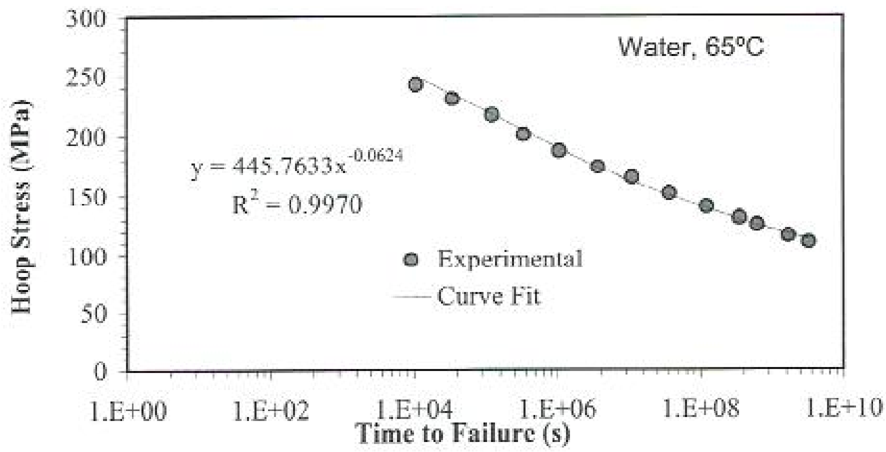

Figure 6.6 Experimental creep failure of pipes at 65°C.

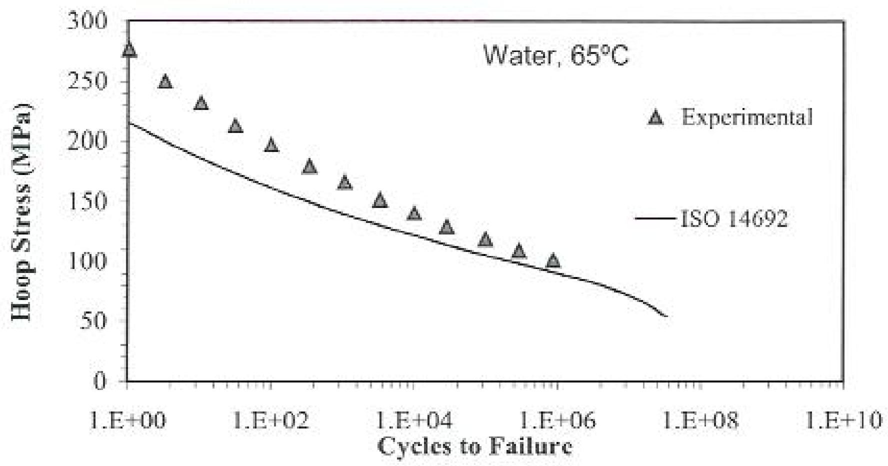

Figure 6.7 Experimental and predictions using creep data (ISO) for fatigue failure of pipes at 65°C.

Hale et al. [38] provide a good account of hygrothermal effects on filament-wound glass fiber-reinforced pipes that were subjected to prolonged exposure to high- temperature water. Two materials systems in common use in offshore piping applications were used, ±55° filament-wound E-glass/phenolic and ±55° filament-wound E-glass/epoxy pipes. The loading modes were hydrostatic pressure with closed and open ends and axial loading. The last mode was produced by applying the same pressure to the interior and exterior of the pipe to eliminate the hoop stress.

Biaxial failure envelopes were obtained for both types of pipe materials in the water-saturated state at a range of temperatures from 20° to 160°C. It was observed that the strength of the epoxy pipes was significantly reduced as temperature increases, especially in the matrix-dominated modes close to pure hoop and pure axial loading. In contrast, the phenolic pipes were unaffected by temperature for all tested modes.

Concerning the application of failure theories to this type of filament-wound pipe, we must note, as a consequence of the wwfe (world-wide-failure-exercise) [39], it is recommended that special care be taken wherever large deformations may be involved. This is especially relevant for ±55° laminates, since none of the failure theories coped very well with these cases.

6.3.2 *Creep rupture*

This section offers an overview of long-term creep failure data for internally pressurized filament-wound pipes. Unfortunately, the available experimental data on creep and creep failure of composite pipes is quite limited.

Mieras [40] described the creep behavior of internally pressurized filament-wound glass-reinforced epoxy and polyester pipes. It was shown how important the resin is for the long-term behavior of the pipes. Creep occurred at all stress levels down to 40 MPa. At higher stresses, creep leads to weeping. In Figure 6.8, long-term weeping stresses are plotted.

The failure mechanism for weepage in filament-wound pipes was described in a great detail by Jones and Hull [41] for two distinct modes, hydrostatic pressure with open and closed ends. The interlaminar cracks associated with transverse matrix cracking tend to grow and intersect, providing paths through the pipe wall for weeping to occur.

Since creep loading at higher stress levels leads to weeping and eventually to total failure, it must be concluded that creep does promote damage comparable to the short-term cracking that was observed for the UEWS (Ultimate Elastic Wall Stress) tests [40] as depicted in Figure 6.9.

Nevertheless, the results reported by Mieras [40] on hoop stress/hoop strain curves were not observed by others, especially by Hull et al. [42]. For mode 2 (hydrostatic pressure with closed ends) the sharp bend in the hoop stress/hoop strain curve was not observed. Hull et al. [42] advanced an explanation, suggesting the phenomenon originated from the step-loading used by Mieras [40].

The UEWS test is used to identify a stress level beyond which permanent deformations are obtained and the material creep rate increases substantially. The UEWS test applies increasing pressure levels based on groups of 10 one-minute hydrostatic pressure cycles [40,43–45]. The procedure consists of performing a series of loading cycles in successive increasingly higher loading steps (10 equal cycles at each level), while measuring the maximum hoop or axial strain obtained

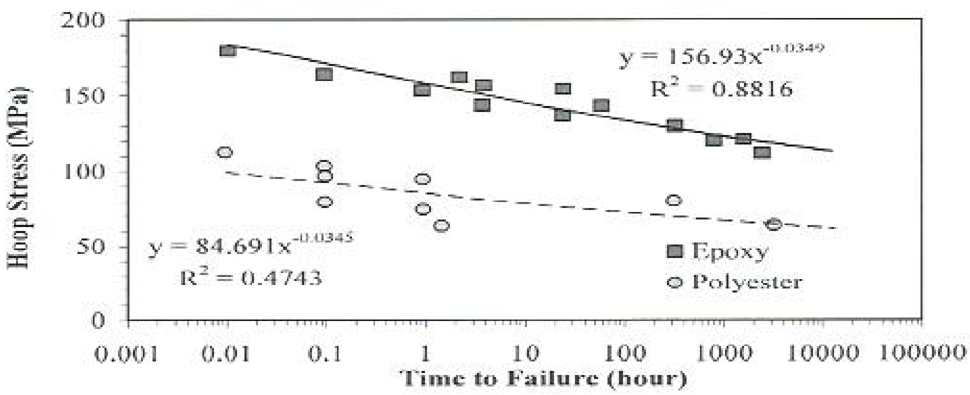

Figure 6.8 Long-term weeping stresses in epoxy and polyester filament-wound pipes (after Mieras [40]).

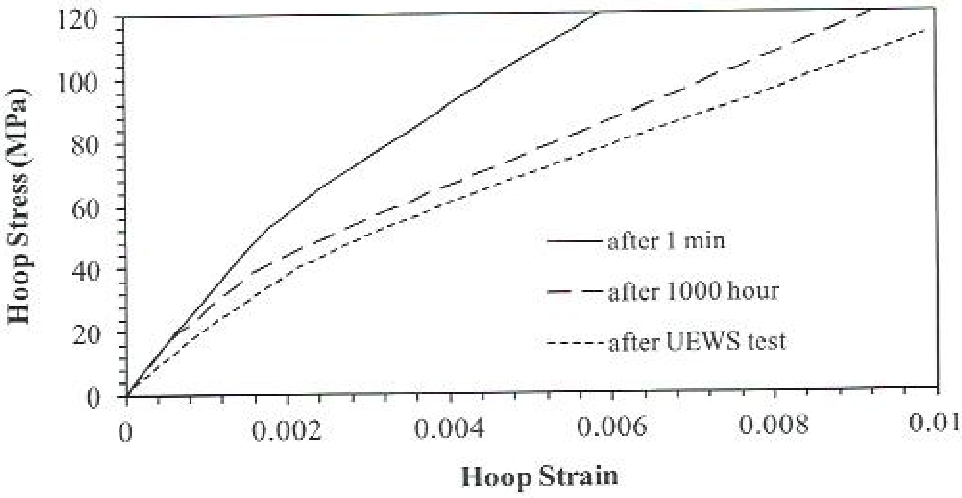

Figure 6.9 Isochronous stress/strain curves for epoxy pipes compared with that of the pipe after Ultimate Elastic Wall Stress (UEWS) tests.

in the first and tenth cycle of each step. The difference between these two strains is used to verify whether elastic limits have been reached. Initially, the pipe specimens are loaded using a hydrostatic pressure up to 10% of the expected UEWS level with the hydrostatic pressure maintained for 1 minute. Then the hydrostatic pressure is released, and the pipe remains unloaded for another minute. This loading-unloading pattern is repeated 10 times with the strains being measured at the end of the first and tenth one-minute load cycle. Subsequently, similar 10-cycle series are successively repeated with the hydrostatic pressure in each step being increased by 10% of the expected UEWS hydrostatic pressure. The test is scheduled to continue until a certain level of permanent deformation is reached (5%).

The UEWS test is a simple procedure that takes a few hours to perform. As Gibson et al. [37] maintain, the UEWS can become an accepted alternative for re-confirming pipe qualification whenever a minor product change is made. The actual procedure for re-confirmation also mandates survival tests with samples held under hydrostatic pressure for 1000 h. Survival in this test leads to a conclusion: the samples tested are at least as good as those originally qualified.

Ghorbel et al. [3, 46] investigated the creep and damage of filament-wound pipes reinforced with E-glass fibers wound at ±55° for two different resin systems: polyester and vinylester. The response of the preconditioned pipes in water at 60°C under sustained hydrostatic pressure with closed-ends was nonlinear viscoelastic. It was observed that creep under hygrothermal conditions induces interlaminar cracking. The time-dependent failure under sustained loading followed a trend similar to that depicted in Figures 6.10 and 6.11.

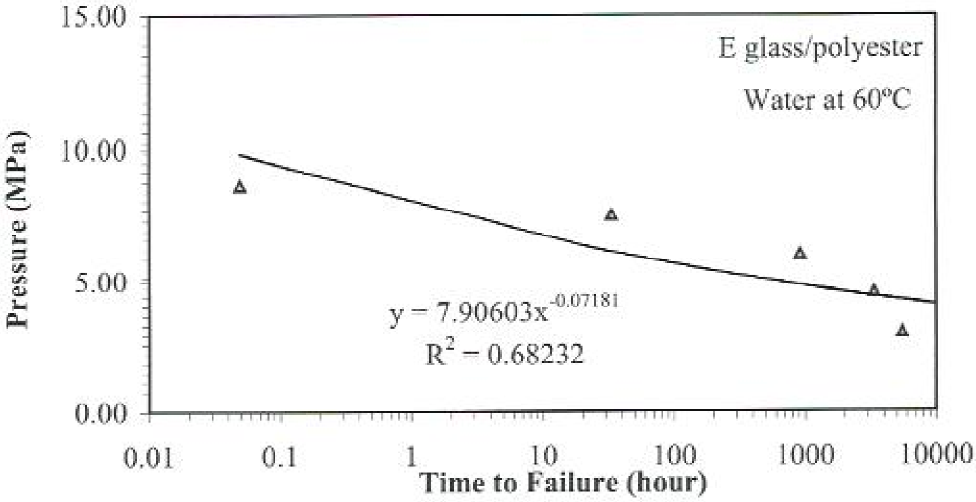

Figure 6.10 Long-term creep failure of E glass/polymers pipes wound at ±55°C immersed in water at 60°C [3].

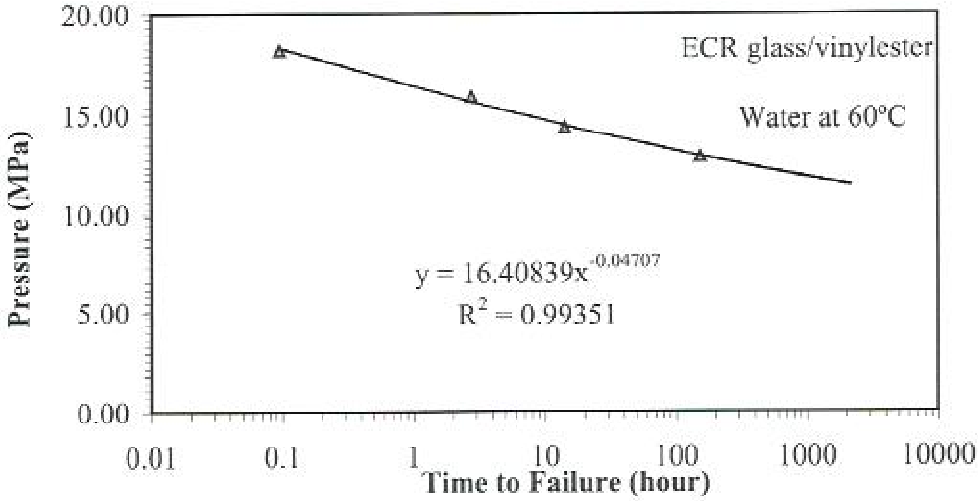

Figure 6.11 Long-term creep failure of E glass/vinylester pipes wound at ±55°C immersed in water at 60°C [3].

It was concluded that the failure mechanisms and time-dependent failure depend strongly on the resin, as can be observed in Figures 6.10–6.11. In contrast to high pressure levels, at low pressure levels the effect of environment must be assessed, since it significantly affects the time-dependent failure.

The determination of the long-term resistance to internal pressure, based on the standard EN1447, which is accomplished by imposing hydrostatic internal pressure on the specimens using axial constrained-free-end sealing devices, was described by Faria and Guedes [47–48]. Figure 6.12 depicts the testing apparatus.

GFRP pipes of three different construction types, from major European manufacturers, were used. The properties of the series of specimens used are displayed in Table 6.1.

Figures 6.13 to 6.16 depict the creep failure curves for each pipe type. It is clear that the pipes' construction and material composition have a strong influence on their long-term behavior, especially when comparing a matrix of epoxy resin and polyester resin (UP). Despite considerable scatter in the tests results, which is usual, statistical regression analysis determined no relevant differences between using complete data (including tests up to 10,000 h) or using only data from shorter tests (up to 1000 h). These long-term hydrostatic tests will be used later in this chapter in a discussion of pipe qualification.

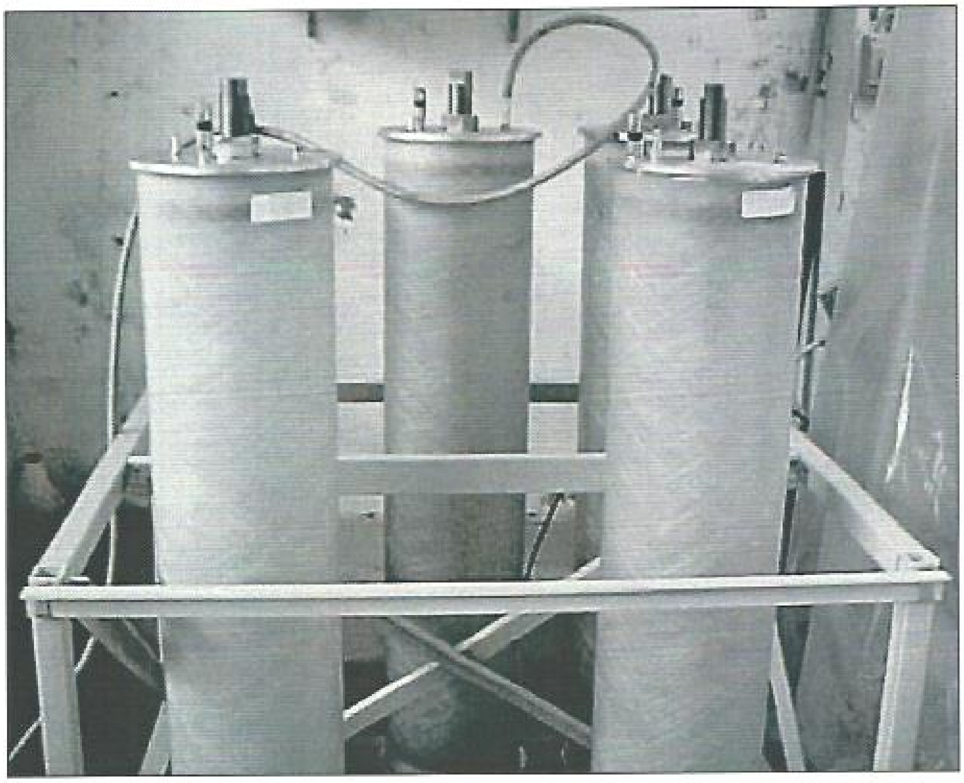

Figure 6.12 Apparatus used in the EN1447 test procedures.

Table 6.1
GFRP pipe specimens used in the experimental test series.

	GFRP pipe type			
	A	B	C	D
Construction Type	filament winding (epoxy)	filament winding (UP)	Hybrid – filament winding + mat deposition (UP)	centrifugal casting (UP)
Nominal Diameter (mm)	300	300	300	300
Nominal Stiffness (N/m²)	5000	5000	5000	5000
Nominal Pressure (bar)	10	10	10	10
Specimen Length (mm)	1300	1300	1300	1300

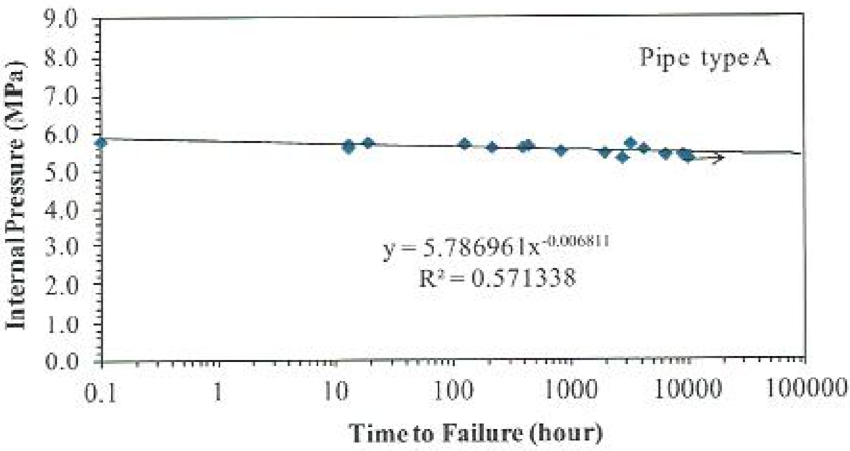

Figure 6.13 Creep failure results for type A pipe.

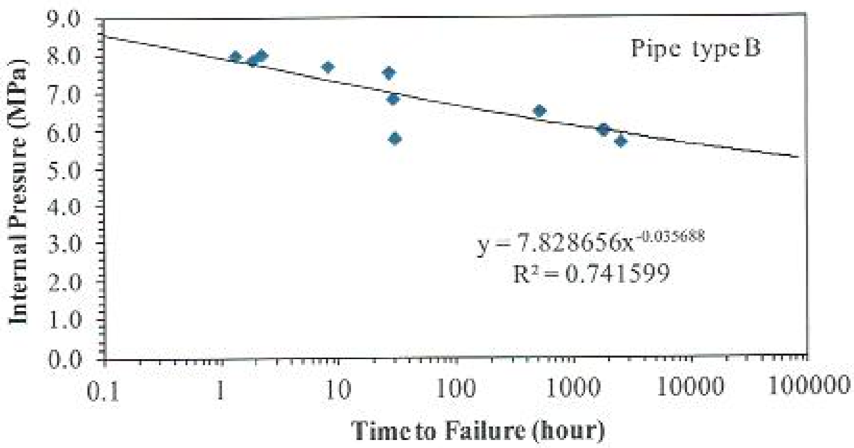

Figure 6.14 Creep failure results for type B pipes.

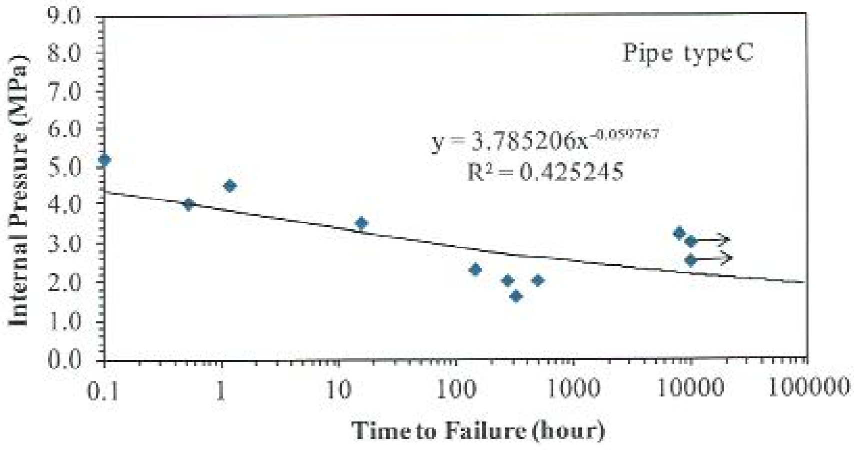

Figure 6.15 Creep failure results for type C pipes.

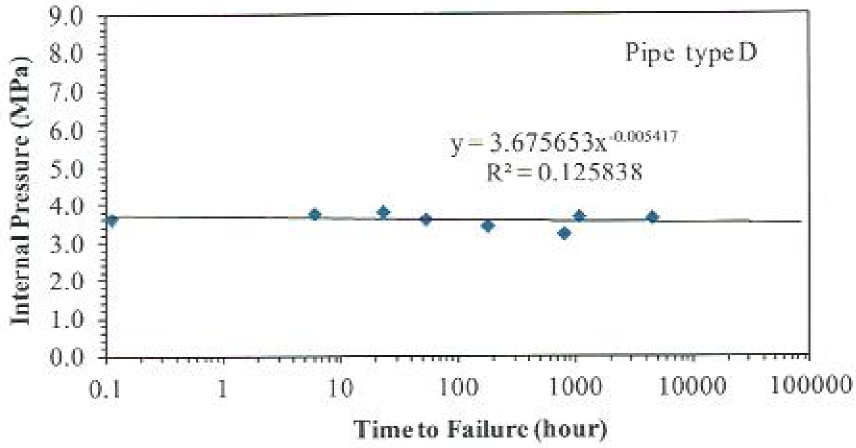

Figure 6.16 Creep failure results for type D pipes.

6.3.3 An example of preliminary design for the long-term

The netting analysis is useful for preliminary calculation of filament-wound pipes under hydrostatic pressure. These structures are primarily loaded in membrane, and that may be considered the simplest case for design. The netting analysis assumes that the stresses induced in the structure are borne entirely by the fibers, and the strength of the resin is neglected. Moreover, it assumes that the fibers possess no bending or shearing stiffness, and carry only the axial tensile loads.

The netting analysis is described in detail in [49–50]. Evans and Gibson [51] obtained analytical expressions for the stress–strain relations from classical laminated plate theory (CLPT) to show the discrepancy between CLPT and the netting theory and reveal significant factors for design. Verchery's [52] approach to the same problem proved to be more effective for deriving explicit design formulas applicable to any state of stress and stacking sequence.

As an example of long-term preliminary analysis, let us suppose we have a ±55° glass/epoxy filament wound pipe with an internal diameter of 100mm and a wall thickness of 5mm, sustaining a hydrostatic pressure of 0.6 MPa. The hoop stress is

$$\sigma_{hoop} = \frac{P_i D}{2t} = \frac{0.6 \cdot 100}{2 \cdot 5} = 6\text{MPa}, \tag{6.33}$$

and axial stress is $\sigma_{axial} = 0.5 \cdot \sigma_{hoop}$

The netting analysis for this condition, with an optimal winding angle of $\arctan\sqrt{2} \cong 54.74°$, assumes that the stress normal to the fibers is null and the stress in the fibers direction is calculated as [53]:

$$\sigma_f = \frac{1}{\sin^2(54.74°)}\sigma_{hoop} \cong 9.0\text{MPa}, \tag{6.34}$$

Now we can calculate the fiber strength, which remains after degradation on a long-term basis [53], i.e., the allowable fiber design strength for the pipe as:

$$\sigma_\alpha = \sigma_v P_t P_{sc} P_s, \tag{6.35}$$

where σ_α is the virgin fiber strength, P_t is the thermal degradation factor, P_{sc} is the stress concentration factor and P_s is the factor for long-term static loading. Let us assume that for the glass fiber we have $\sigma_\alpha = 157\text{MPa}$. The strength reduction due to thermal degradation is assumed as $P_t = 0.8$. After the fiber is placed in the strand, the strength tensile reduction is about 25%, i.e., $P_{sc} = 0.75$, due to localized stress concentrations, fiber crossovers and residual stress, among others. Since glass fibers are particularly susceptible to static fatigue effects (creep), in many cases the strength reduction due to long-term static loading is very high, i.e., $P_s \in [0.1, 0.2]$ [53]. Assuming in this case $P_s = 0.1$, the allowable fiber design strength becomes:

$$\sigma_\alpha = 157(0.8)(0.75)(0.1) \cong 9.4\text{MPa}, \tag{6.36}$$

This residual strength is slightly larger than the fiber stress calculated from the netting analysis, which indicates a reasonable long-term preliminary design.

6.4 LIFETIME OF COMPOSITES PIPES UNDER CYCLIC LOADING

Polymers and polymer-based composites fail, given enough time, when submitted to cyclic loads at stresses well below their static failure loads. This phenomenon is called fatigue. The typical approach to fatigue is to develop fatigue curves, i.e., applied stress (S) against the number of cycles until failure (N). These curves are usually designated as S-N curves and resemble a sigmoid function, displaying a stress limit for large cycles, suggesting a fatigue limit. Moreover the S-N curves for polymers and polymer based composites are extremely frequency dependent.

As many research works have shown, cyclic loading can significantly degrade the stiffness and strength of pipes. Frost [54] and Frost and Cervenka [43] obtained the S-N (fatigue) curves of ±55° glass-fiber/epoxy filament wound pipes with 100mm internal diameter (14 MPa rated pressure). The curves were fitted using the power law expressed as:

$$\log(P) = A - B\log\left(\frac{t}{\tau_0}\right) \tag{6.37}$$

where P is the pressure (or hoop stress or axial stress), t the time, and τ_0 the reference time. The curves are extrapolated for 20 years to define the long-term hydrostatic pressure (LTHP). The resulting value is multiplied by a number of factors (typically 0.5 [43]), resulting in a pressure known as the hydrostatic design basis (HDB) [44].

Tarakcioglu et al. [55] tested ±55° glass-fiber/epoxy filament-wound pipes under internal pressure. The pipes had four layers with 1.6 mm in thickness, 300mm in length and an inner diameter of 72mm. Stress levels were 30% (121.5 MPa), 35% (141.7 MPa), 40% (162 MPa), 50% (202.5 MPa), 60% (243 MPa) and 70% (283.5 MPa) of the static strength of the specimen (405 MPa). Sinusoidal stress levels were applied at 0.42 Hz for R = 0.05 stress ratio (R = Maximum stress/Minimum stress). Fatigue results were recorded for three different damage stages, namely, whitening, leakage and final failure. The three stages of whitening (fiber/matrix interface debonding and delamination), leakage initiation, and final failure occurred sequentially. Micrographs from an SEM observation proved that there is an analogy between the macro-damage stages and the micro-damage mechanisms. It is possible to fit equation (6.37) to the three damage stages shown in Figures 6.17–6.19 with a very good correlation. For all stress levels, ultimate failure occurred almost immediately after leakage initiation.

Another study of E-glass/epoxy filament-wound pipes of four layers with a ±75° winding angle, using the same test conditions, led to similar conclusions [56]. In both cases no evidence of a fatigue limit was found.

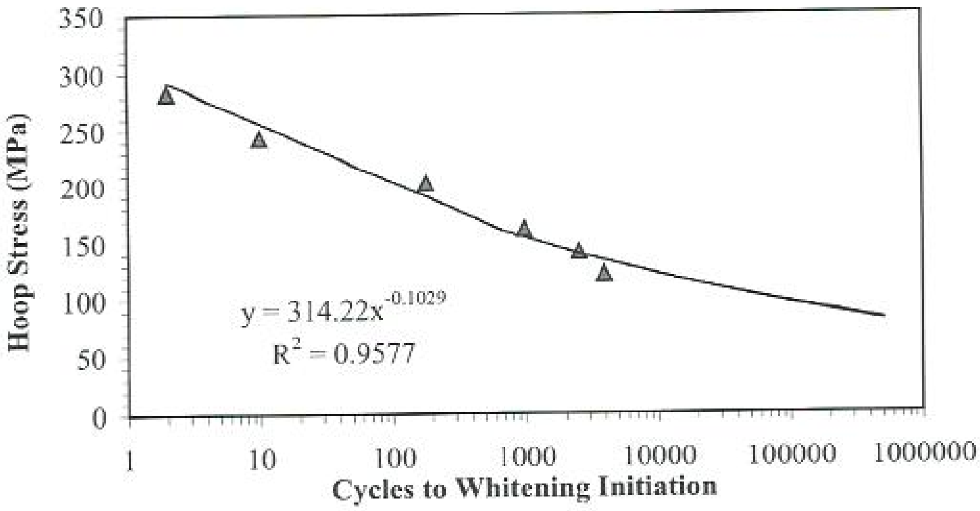

Figure 6.17 S–N curve for whitening initiation of ±55° glass-fiber/epoxy filament-wound pipes.

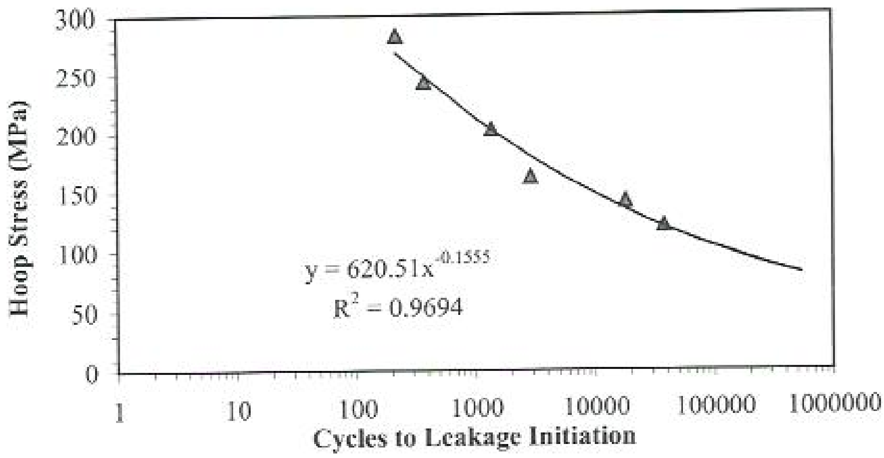

Figure 6.18 S–N curve for leakage initiation of ±55° glass-fiber/epoxy filament-wound pipes.

Fatigue under biaxial loading was obtained by Perreux and Joseph [57] for E-glass/epoxy pipes with four layers with ±55° winding angle. The pipes had a diameter of 60mm and a length of 2800mm and were cut into 350mm lengths. The fatigue tests were done under three different modes: hydrostatic pressure with closed and free ends and axial tensile loading.

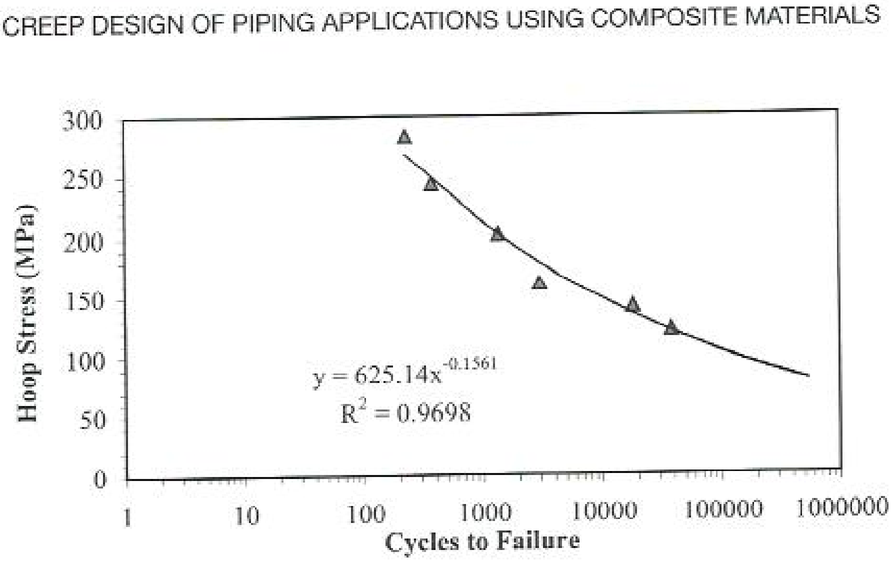

Figure 6.19 S–N curve for final failure of ±55° glass-fiber/epoxy filament-wound pipes.

The results are summarized in Figures 6.20–6.22.

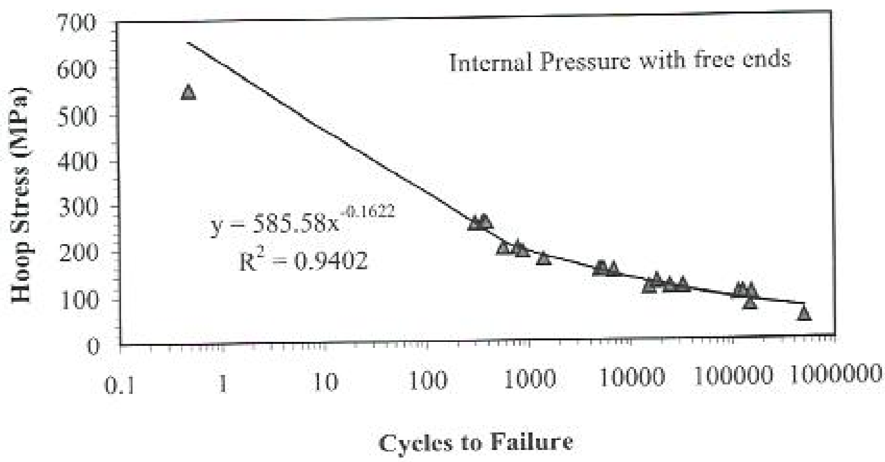

Figure 6.20 S–N curve for final failure of ±55° E-glass/epoxy filament-wound pipes under hydrostatic pressure with free ends for a frequency of 0.2 Hz.

The previous results can be put in the form of an isonumber of cycles to failure, depicted in Figure 6.23. This provides an approximate idea of the evolution of failure envelopes with cycle fatigue. Hence, in this case, the failure envelope for 10^6 cycles can be obtained from the static failure envelope by applying a scaling factor of 0.1.

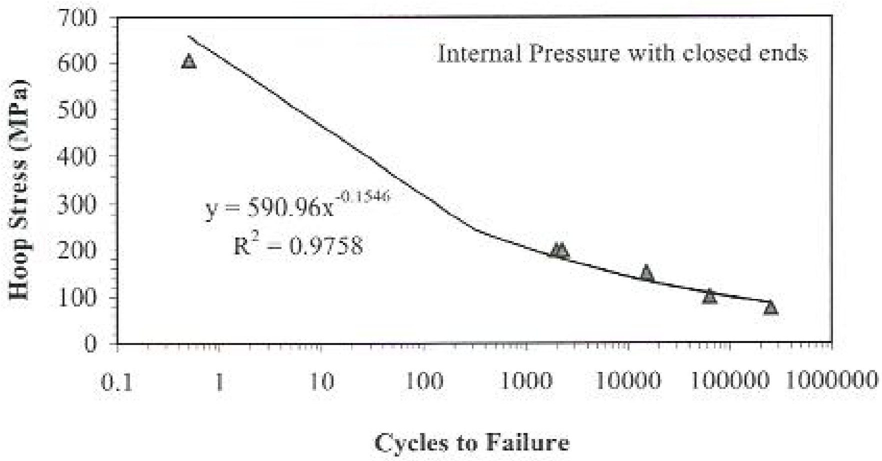

Figure 6.21 S–N curve for final failure of ±55° E-glass/epoxy filament-wound pipes under hydrostatic pressure with closed ends for a frequency of 0.2 Hz.

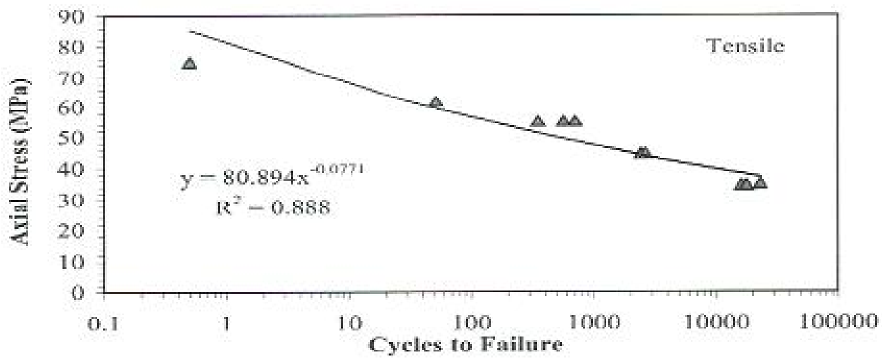

Figure 6.22 S–N curve for final failure of ±55° E-glass/epoxy filament-wound pipes under axial tensile load for a frequency of 0.2 Hz.

The effect of frequency on fatigue lifetime was also studied by Perreux and Joseph [57]. It was concluded that fatigue lifetime does increase with frequency from 0.2 to 1Hz, i.e., 2–3 fold higher. Later, Perreux and Thiebaud [58] concluded there are two concurrent phenomena that influence fatigue failure: (1) interaction between creep and fatigue at low frequency, which increases the lifetime when the

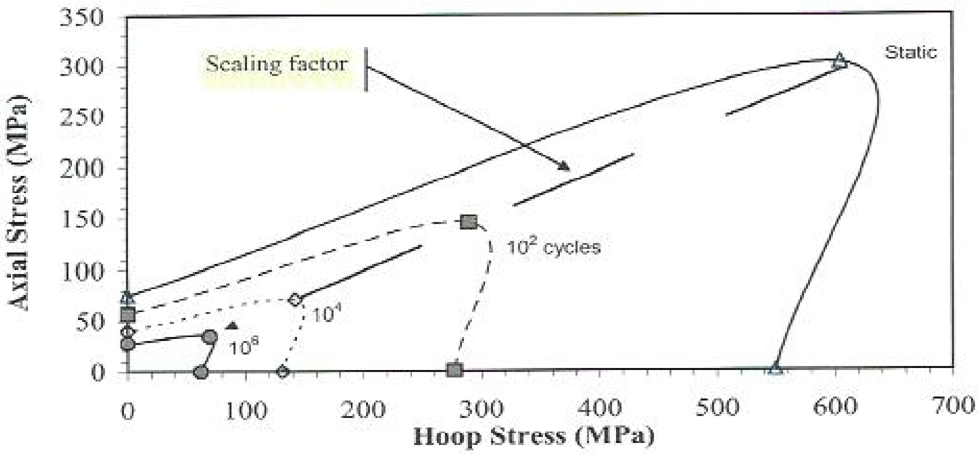

Figure 6.23 Failure envelopes for ±55° E-glass/epoxy filament-wound pipes under biaxial tensile load, for multiple fatigue cycles.

frequency is increased, and (2) a thermal effect due to viscoplastic dissipation at a higher frequency, which reduces the lifetime when the frequency is increased. Thus, all situations can be observed, depending on which phenomena are most intense. It should be noted that there is no effect of the frequency on the lifetime if the phenomena have similar intensity. However, this result shows that a material's lifetime as measured in fatigue can depend on the shape of the specimen as well as on thermal dissipation.

Ellyin and Martens [59] investigated the multi-axial fatigue of pipes, showing that there are two stages in failure: a functional one and final structure rupture. Kaynak and Mat [60] studied tensile fatigue and showed that damage has three stages: crack initiation, crack growth and concentration along the fibers' direction, and fiber failure. They also studied the effect of frequency on fatigue lifetime and concluded, as Joseph and Perreux [57] had, that the tensile fatigue lifetime increases with frequency.

In conclusion, the effect of cycling loading on damage initiation and propagation is more severe than sustained loading, i.e., creep loading. The UEWS tests, previously mentioned and described, are strongly linked to fatigue tests as was demonstrated by Gibson et al. [37]. A simple simulation of a UEWS test can be done, using creep and fatigue failure curves from [37], to compute the cumulative damage that originated separately from creep and fatigue. This was accounted for using Miner's law as suggested in [37]. The calculations are depicted in Figure 6.24. It is quite obvious that in the UEWS test the fatigue effect on damage is much more pronounced.

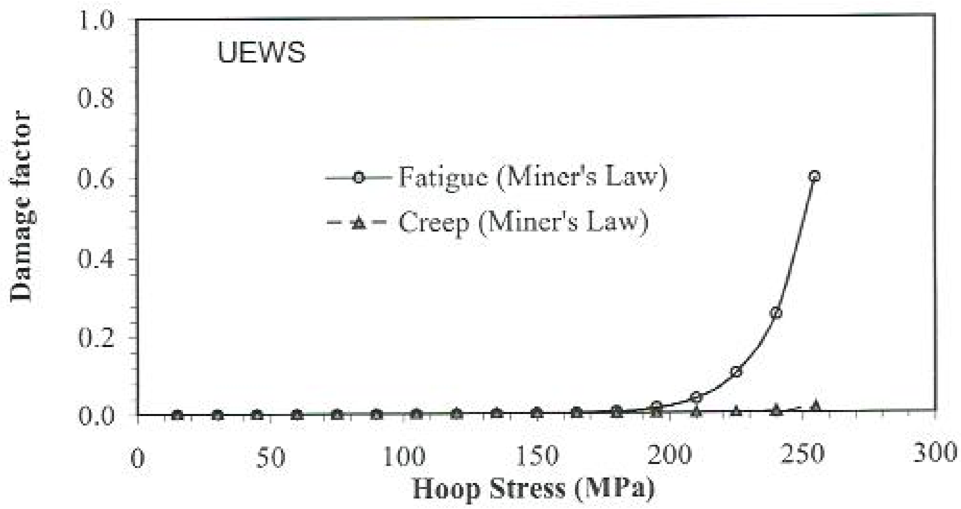

Figure 6.24 Computed Miner's law sum, for creep and fatigue, at each hoop stress level in the UEWS test.

6.5 APPLICABLE STANDARDS

6.5.1 6.51 Identification and comparison of main standards

Among the increasing range of applications where glass-fiber-reinforced plastic (GRP) pipes are used, oil/gas and sewage transportation are the most relevant. For the former, internal pressure is considered to be the representative and governing loading condition. Therefore, the product and test standards specify design and qualification criteria based on this loading case. Sewage pipe are treated mostly as a low-pressure application, and thus reduced qualification criteria may be adopted. Also, whether the pipe is above- or underground determines the type of external supports and the conditions to which the pipes are subjected during their in-service life time. This also can lead to changes in design and qualification procedures.

Despite the fact that highly specific requirements may be needed for each individual piping application, the major standardization organizations worldwide have developed product and test standards that strive to cover the most common applications. Namely, ASTM International (formerly known as the American Society for Testing and Materials), AWWA—American Water Works Association, CEN—the European Committee for Standardization and ISO—International Organization for Standardization have all published multiple standards comprising guidelines for both manufacturers and end-users of GRP piping systems. During the last 25 years, such normative references have evolved from the initial, empirically-based conservative approaches to a combination of experimental and statistical analyses, which nonetheless are also empirical. Hence, these standards have established a baseline for the design, manufacture, qualification, installation and operation of GRP piping systems (i.e., pipes, fittings and related accessories).

In Table 6.2, a comparison of the required/preferred procedures of the main GRP pipe product standards is presented. The standards for the product-types mentioned below [54–59] are compared:

- ASTM D3262—Standard Specification for "Fiberglass" (Glass-Fiber-Reinforced Thermosetting-Resin) Sewer Pipe.
- ASTM D3517—Standard Specification for "Fiberglass" (Glass-Fiber-Reinforced Thermosetting-Resin) Pressure Pipe.
- ASTM D3754—Standard Specification for "Fiberglass" (Glass-Fiber-Reinforced Thermosetting-Resin) Sewer and Industrial Pressure Pipe.
- ASTM D2997—Standard Specification for Centrifugally Cast "Fiberglass" (Glass-Fiber-Reinforced Thermosetting-Resin) Pipe.
- AWWA C950—Standard for Fiberglass Pressure Pipe.
- AWWA M45—Fiberglass Pipe Design Manual.
- EN 1796—Plastics piping systems for water supply with or without pressure—Glass-reinforced thermosetting plastics (GRP) based on unsaturated polyester resin (UP).
- EN 14364—Plastics piping systems for drainage and sewerage with or without pressure—Glass-reinforced thermosetting plastics (GRP) based on unsaturated polyester resin (UP)—Specifications for pipes, fittings and joints.
- ISO 10467—Plastics piping systems for pressure and non-pressure drainage and sewerage—Glass-reinforced thermosetting plastics (GRP) systems based on unsaturated polyester (UP) resin,
- ISO 10639—Plastics piping systems for pressure and non-pressure water supply—Glass-reinforced thermosetting plastics (GRP) systems based on unsaturated polyester (UP) resin.
- ISO 14692—Petroleum and natural gas industries—Glass-reinforced plastics (GRP) piping.

These standards are cited because they form the current references for industry and end-users worldwide. Each group of product standards (ASTM, AWWA, EN and ISO) covers: pressure and non-pressure, aboveground and underground, offshore and onshore applications of GRP pipes. Although they are suitable for GRP pipes manufactured by different processes (filament winding, centrifugal casting, hand lay-up etc.), and with different matrix materials (polyester, vinyl-ester and epoxy resins), each refers to a specific manufacturing process and material configuration as the basis for the design and qualification methodology stated in it.

ASTM D3517, AWWA C950, EN 1796 and ISO 10639 are alternatively used mainly for water supply piping systems with in-service internal pressure loading conditions. ASTM D3262, ASTM D3754, EN 14364 and ISO 10467 are alternatively used mainly for sewage transportation piping systems where no internal

Table 6.2
Identification and comparison of GRP pipe standards.

Test/Parameter	Standard										
	ASTM D3262	ASTM D3517	ASTM D3754	ASTM D2997	AWWA C950	AWWA M45	EN 1796	EN 14364	ISO 10467	ISO 10639	ISO 14692
Initial circumferential tensile strength (failure pressure)	n/a	ASTM D1599	ASTM D1599	ASTM D1599	ASTM D1599	ASTM D1599	EN 1394	EN 1394	ISO 8521	ISO 8521	ASTM D1599
Long-term circumferential tensile strength (failure pressure)	n/a	ASTM D2992	ASTM D2992	ASTM D2992	ASTM D2992	ASTM D2992	EN 1447	EN 1447	ISO 7509	ISO 7509	ASTM D2992
Cyclic pressure strength	n/a	n/a	n/a	ASTM D2143	ASTM D2143	ASTM D2143	EN 1638	EN 1638	ISO 15306	ISO 15306	ASTM D2143
Initial specific ring stiffness	ASTM D2412	ASTM D2412	ASTM D2412	ASTM D2412	ASTM D2412	ASTM D2412	EN 1228	EN 1228	ISO 7685	ISO 7685	ASTM D2412
Long-term specific ring stiffness	n/a	n/a	n/a	n/a	n/a	n/a	ISO 10468	ISO 10468	ISO 10468	ISO 10468	n/a
Initial ring deflection	ASTM D2412	ASTM D2412	ASTM D2412	n/a	ASTM D2412	ASTM D2412	ISO 10466	ISO 10466	ISO 10466	ISO 10466	ASTM D2412
Long-term ring deflection	n/a	n/a	n/a	n/a	n/a	n/a	ISO 10471	ISO 10471	ISO 10471	ISO 10471	n/a
Longitudinal tensile strength	ASTM D638	ASTM D638	ASTM D638	ASTM D2105	ASTM D2105	ASTM D2105	EN 1393	EN 1393	ISO 8513	ISO 8513	ASTM D2105
Methods for regression analysis of test data	n/a	(ASTM D2992)	(ASTM D2992)	(ASTM D2992)	(ASTM D2992)	(ASTM D2992)	ISO 10928	ISO 10928	ISO 10928	ISO 10928	(ISO 14692)

pressure is considered. ISO 14692 is broadly used in the oil and gas industries, mainly for off-shore applications. Since it covers the design and qualification of suspended pipe systems, AWWA M45 is often complimentarily used for underground pipe systems within the same industries.

The main differences between ISO 14692 and the other ISO and CEN product standards for pressure piping applications are that:

- the regression qualification procedure is based on a design life of 20 years (approx. 175,400 hours), instead of 50 years (approx. 438,000 hours);
- the full regression qualification procedure requires only 18 specimens to be tested, instead of 23 specimens;
- it provides default values for the slope of the regression line for preliminary design calculations and/or determination of test conditions (in cases where there is no data);
- it allows a breakdown of a product family into family representatives, product sectors, component variants and product sector representatives in order to reduce the overall quantity and duration of the qualification tests; in this way, only the family representatives are required to pass through the full qualification procedure while the other variants have to pass only a 1000 h survival test (ASTM D1598);
- it establishes a normative procedure to determine the factored failure envelope, considering a biaxial (hoop plus axial) stress state (Figure 6.25);
- the reference test temperature is 65°C, instead of room temperature;
- it establishes a limited (less stringent) qualification procedure for low-pressure water applications.

As can readily be observed in Table 6.2, the standard ISO 14692 adopted the ASTM methodology and thus allows for design and qualification procedures that are less expensive and time-consuming than other ISO and CEN standards. Nevertheless, the ISO 14692 procedure retains a conservative quality by: (1) requiring higher test temperatures (thus aging the specimens during the tests) and (2) using a lower confidence-limit level to determine the long-term hydrostatic pressure (instead of directly extrapolating from the regression line).

In order to assess the regression line that permits the prediction of the long-term hydrostatic pressure or hoop stress level that leads to a lifetime of 20 years (ISO 14692) or 50 years (EN 1796), the critical procedure lies within the standards tests ASTM D2992 or EN 1447, respectively. These standards establish the procedures for obtaining the hydrostatic design basis (HDB) or the pressure-design basis (PDB) for GRP piping products, by evaluating strength-regression data derived from pipe or fittings tests. The data obtained from these test methods is plotted as hoop stress or internal pressure versus time-to-failure relationships at the selected temperatures that simulate actual anticipated product end-use conditions. This practice defines a hydrostatic design basis (HDB) for material in straight, hollow

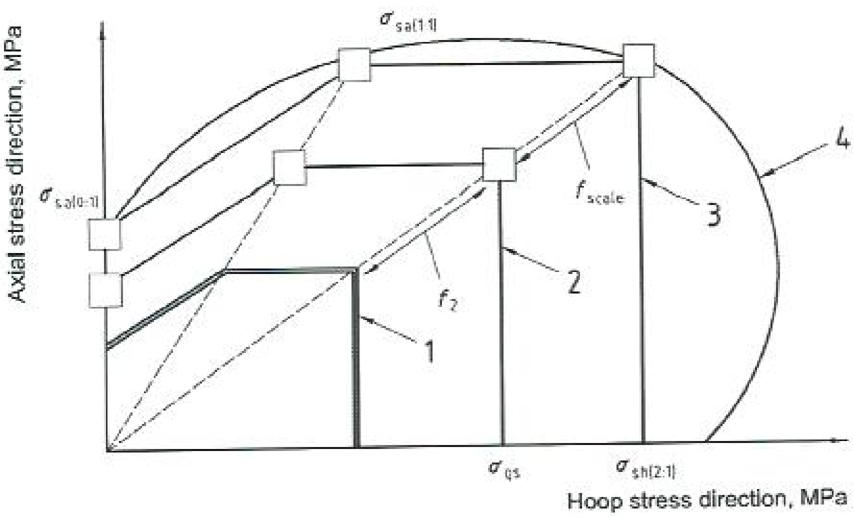

Figure 6.25 Idealized envelopes for a single-wound angle-ply GRP pipe with winding angles ranging from 45° to 75°. (1) long-term design envelope, (2) idealized long-term envelope, (3) idealized short-term envelope, (4) schematic representation of the short-term failure envelope (after ISO 14692:2002).

cylindrical shapes where hoop stress can be easily calculated, and a pressure-design basis (PDB) for fittings and joints where stresses are more complex.

ASTM D2992, in particular, includes two test procedures, accounting for two typical in-service loading cases (not limited to internal pressure):

- Procedure A—a minimum of 18 specimens of pipe (or fittings) are placed under cyclic internal pressures at a cycle rate of 25 cycles per minute, at several different pressures. The stress or pressure values for the test are selected to obtain a proper distribution of failure points in the time decades (in log scale). The cyclic long-term hydrostatic strength (LTHS) of a pipe is obtained by an extrapolation of a log-log plot of the linear regression line for hoop stress versus cycles to failure.
- Procedure B—a minimum of 18 specimens of pipe (or fittings) are placed under constant internal pressures at different pressure levels in a controlled temperature environment. The time-to-failure for each pressure level is recorded. The stress or pressure values for the test are selected to obtain a proper distribution of failure points along the time decades (in log scale).

EN 1447 is truly identical to ASTM D2992, differing only in the long-term time objective (50 years instead of 20 years) and thereby requiring a greater number of specimens so that the extrapolation can be done with the same statistical confidence level. Both standards methods implicitly assume that the mechanisms responsible for long-term failure are the same at different levels of load and from short- to long-term. Although this limitation is not explicitly addressed in the standards, the experimental evidence of the whole failure phenomenon and the lack of adequate information were the main reason for extending the test periods to over 10,000 hours. In a logarithmic time scale, 10,000 hours is only 1.2 and 1.6 decades distant from 20 years and 50 years, respectively. This makes the existing test and prediction methods seem reasonable.

In the following section a practical case is presented where the regression analysis procedure for long-term hydrostatic pressure is directly applied and the results are discussed.

6.5.2 Long-term qualification tests of four different types of GRP

Two typical in-service load conditions for GRP piping systems are internal pressure and ring deflection. For these, empirical test methods have been developed and are described in the standards ISO 7509:2000 (equivalent to EN 1447:2009) and ISO 10471:2003 (replacing EN 1227:1997), respectively.

The lack of completely understood failure mechanisms and long-term materials performance knowledge necessarily leads to conservative over-estimation and consequently to over-design of the pipe structures. The existence of various types of GRP pipe construction, namely filament wound, centrifugal cast, and hybrid ones, also inhibits any relaxation of test specifications.

Experimental results from standard test procedures, according to EN 1447:2009 and ISO 10928:2009 (which replaced EN 705:1994), conducted on GRP pipes of four different types and respective data analysis are presented below.

The test procedure specified in EN1447 relates to the creep behavior of GRP pipes and requires constant internal pressure loading conditions to be imposed at different levels and during different periods of time on each specimen. The time periods range from a few minutes up to 10,000 hours. Unlike other normative procedures (such as ISO 14692), the test temperature is room temperature. The long-term resistance to internal pressure is determined by imposing hydrostatic internal pressure on the specimens using axial constrained-free end sealing devices. Failure must occur within a determined valid failure zone (in the middle of the specimen) in order to be validated. Time-to-failure is registered. In Figure 6.12 the testing apparatus used in the experimental tests for internal pressure property analysis is depicted.

In this test series, GRP pipes of four different construction types, from four main European manufacturers, were used. The properties of the series of specimens used are indicated in Table 6.1, in section 6.3.

All tests showed considerable scatter in results, which is typical given the material variability of these composite constructions. Different levels of admissible loading and different trends in the results were also observed for GRP pipes that varied in their construction.

The statistical treatment of the data according to ISO 10928:2009 confirmed that only data from campaigns A and B were suitable for extrapolation. However, the experimental procedure showed the data to be applicable to all of the different types, if a few more specimens had been tested in campaigns C and D. Graphic representation of the data is shown in Figure 6.26, accomplished by plotting pressure loading versus time-to-failure in log-log scales. The regression trend lines are also plotted.

From these results several conclusions may be drawn:

- filament-wound pipes are more resistant than the other construction types to structural degradation when subjected to constant internal pressure. This is observed from the smaller slope of the regression lines of pipes A and B;
- pipes of type A, made with epoxy resin, displayed very consistent behavior for all test periods, suggesting that this resin system might be less vulnerable to moisture absorption and softening by resin-fiber de-cohesion and general degradation;
- pipes of type C, manufactured by a hybrid combination of filament winding (continuous fibers) and mat deposition (short fibers), with relevant inclusions of silica, showed a very steep slope, thus displaying an overall degradation rate much higher than the others. The lack of a continuous reinforcement surely increases the creep factor of the structure, since only the resin permanently sustains circumferential stress;

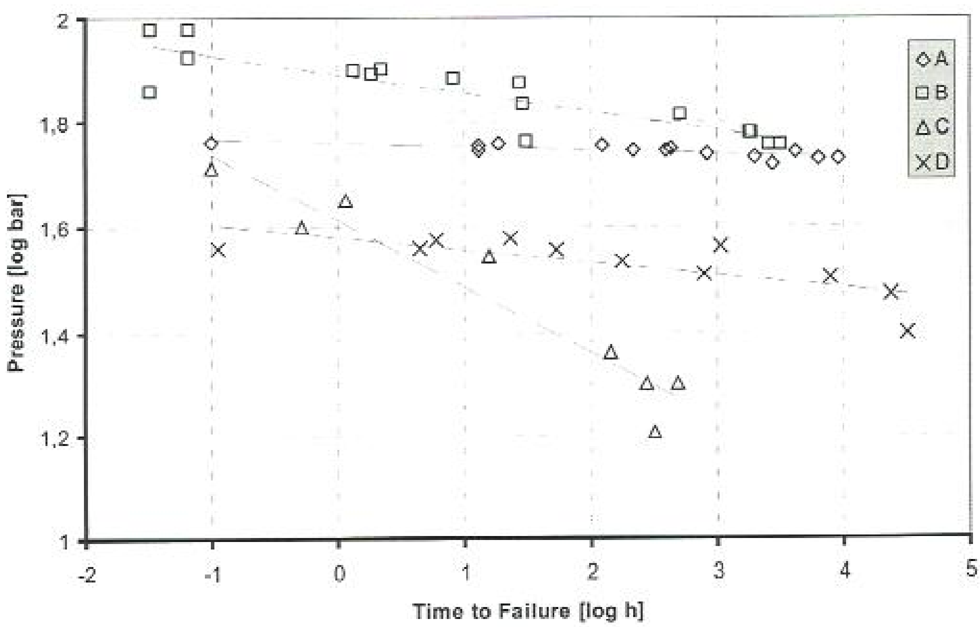

Figure 6.26 Results of the test series conducted accordingly to EN 1447:2009 – pressure versus time-to-failure in log-log scale [59].

- pipes A, C and D show very similar short-term results, which agrees with their equal nominal specifications, namely, initial stiffness and strength, since they are classified for the same nominal service pressure and ring stiffness. Specimens of type B seem clearly to be over-designed for the specific application of internal pressure.

6.6 PRACTICAL DESIGN: A CASE STUDY

In this section, a practical design case is addressed in accordance with ISO 14692:2002 [54]. In the example, material and experimental short-term failure test data are used to estimate the long-term failure envelope of a specific GRP pipe type. The nominal pressure rating of such a pipe system is then determined by following the design procedure established in the referenced standard for a design life of 20 years.

In order to correlate this practical example with real applications within the oil & gas fields, as well as with the previous experience gathered from the experimental tests summarized in Figure 6.26, a glass-fiber reinforced epoxy (GRE) pipe system was selected. The properties of a filament-wound GRE pipe with two ±55° layers, characterized by Soden et al. [35], were considered. The type of construction and geometry of the pipes are presented in Table 6.3. The mechanical properties for each of the four single-angle laminae are summarized in Table 6.4.

Since no specific long-term test data is available for the selected pipe specimens, the test data obtained for the pipe specimens of type A in Figure 6.26 has been used, in order to establish a reasonable long-term hydrostatic pressure, p_{LTHP}, as a reference for the design procedure.

Table 6.3
Main specifications of the GRE pipe specimens considered in the practical design case [35].

Construction Type	Filament Winding
fibre type	Silenka E-glass 1200TEX
resin type	MY750/HY917/DY063 epoxy
winding angle [°]	±55
number of ± plies	2
internal diameter (DN) [mm]	100
average wall thickness [mm]	1
fibre volume fraction [%]	60
post-curing cycle	2 h @ 90°C + 1.5 h @130°C + 2 h @ 150°C

Table 6.4
Mechanical properties of each single-angle (+55° or −55°) lamina of GRE pipe specimens considered in the practical design case [35].

axial modulus [GPa]	39.4
circumferential modulus [GPa]	46.6
axial tensile strength [MPa]	767
axial compressive strength [MPa]	578
circumferential tensile strength [MPa]	1071
circumferential compressive strength [MPa]	739

In fact, type A pipe specimens are similar to the ones selected here, both in terms of the applied materials (E-glass fiber and epoxy resin) and manufacturing technique (filament winding). Hence, the absolute value of the slope/gradient, $G = 0.0069$, of the regression line observed in the tests mentioned above (Fig. 6.26, etc.) can constitute a reference for the expected degradation of the properties of the pipes under consideration. However, since the tests presented in Figure 6.26 were conducted at room temperature (EN 1447 [59]) instead of at the higher temperature specified in ISO 14692 [54], the gradient considered hereafter is five (5) times higher than that one. Thus, the absolute value of the gradient of the idealized regression line is conservatively given by:

$$G = 5 \times 0.0069 = 0.0345 \tag{6.38}$$

which corresponds to an estimated degradation of the overall properties of approximately 34% during the 20 years of its useful life. The expected minimum long-term hydrostatic pressure, p_{LTHP}, for the selected pipe is given by:

$$p_{LTHP} = \frac{2t\left(\sigma_{sh}^{u} \times 0.66\right)}{D} = 14.137\ MPa = 141.37\ bar \tag{6.39}$$

where σ_{sh}^{u} is the short-term hoop (circumferential) ultimate strength of the pipe specimen according to the material property data provided in Table 6.4, and t and D are the mean wall thickness and diameter of the pipe specimens, respectively.

For the sake of simplicity, the qualifying pressure, p_q, is herewith assumed to be equal to p_{LTHP}.

The pressure rating to provide in the product literature is given by:

$$p_{NPR} = f_2\ f_3\ p_q \tag{6.40}$$

where f_2 is defined as the part load factor and f_3 is a factor accounting for the limited axial load capability of GRP/GRE pipes. Default values for f_2 are given in ISO 14692 [54] depending on the load-type assessment that is to be considered for the application. These values are 0.67 for the case of sustained loads (pressure, mass, etc.) excluding thermal effects and 0.89 for the combination of sustained loads and occasional loads (water hammer, blast, etc.). Since our assessment is based on sustained internal pressure (with eventual minor induced axial stress), a value of $f_2 = 0.67$ is used.

For further assessments, let us assume that the biaxial stress ratio, circumferential stress/axial stress, of the application and installation for which this pipe is being designed is 1:1 and that the non-pressure-induced axial stress is $\sigma_{ab} = 5\ MPa$.

For the calculation of f_3, the biaxial strength ratio, r, must be assessed using equation (6.40):

$$r = 2\frac{\sigma_{sa(0:1)}}{\sigma_{sh(2:1)}} \tag{6.41}$$

where $\sigma_{sa(0:1)}$ is the short-term axial strength under axial loading only and $\sigma_{sh(2:1)}$ is the short-term hoop (circumferential) strength under 2:1 stress conditions. Within the scope of the World Wide Failure Exercise, Soden et al. [36] presented extensive results for the failure of GRP/GRE pipes under biaxial stress conditions. Table 6.5 lists the failure data points for the ±55° GRE pipe considered in this practical example. These pairs of hoop/axial stress at failure data points define the short-term failure envelope as shown later.

From these results one can easily calculate r by using the averaged values of $\sigma_{sa(0:1)} = 68\ MPa$ and $\sigma_{sh(2:1)} = 736\ MPa$ that these authors found for the specific pipe under consideration. Hence, the value of the ratio r is

$$r = 2\frac{\sigma_{sa(0:1)}}{\sigma_{sh(2:1)}} = 2\frac{68}{736} \approx 0.185 << 1 \tag{6.42}$$

Since $r < 1$, then f_3 is given by:

$$f_3 = 1 - \frac{2\,\sigma_{ab}}{r\, f_2\, \sigma_{fs}} \tag{6.43}$$

where σ_{ab} is the non-pressure-induced axial stress and σ_{fs} is the qualified stress, which is related to the factored qualified pressure, p_{qf}, by the following relation:

$$\sigma_{fs} = \frac{p_{qf}\, D}{2\, t} \tag{6.44}$$

Table 6.5
Biaxial failure test results of thin ±55° GRE pipes subjected to combined internal pressure and axial loading [36].

Hoop Stress [MPa]	Axial Stress [MPa]	Stress Ratio [hoop:axial]	Hoop Stress [MPa]	Axial Stress [MPa]	Stress Ratio [hoop:axial]	Hoop Stress [MPa]	Axial Stress [MPa]	Stress Ratio [hoop:axial]
0	74	0:1	741	370	2:1	761	138	11:2
0	62	0:1	717	358	2:1	676	67	10:1
107	143	3:4	750	375	2:1	516	0	1:0
198	198	1:1	835	334	5:2	594	0	1:0
331	280	6:5	803	321	5:2	638	0	1:0
374	288	13:10	914	305	3:1	622	0	1:0
525	332	3:2	939	283	13:4	544	0	1:0
599	349	7:4	867	262	13:4	492	-27	
723	365	2:1	921	263	7:2	256	-65	
736	368	2:1	817	148	11:2			

The factored qualified pressure, p_{qf}, is related to the qualified pressure, p_q, as follows:

$$p_{qf} = A_1\ A_2\ A_3\ p_q \tag{6.45}$$

where A_1, A_2 and A_3 are, respectively, the partial factors for temperature, chemical resistance, and cyclic service. These additional factors account for specific service conditions that eventually cannot be considered in the qualification program.

Since the operating temperature that one posits for the present example is less than or equal to 65°C, $A_1 = 1$. It is also assumed that the resin is chemically compatible with the operating fluid and therefore $A_2 = 1$. Given the nature of the present study and the typical applications of such GRP pipes, it is supposed that the predicted number of pressure or other cycles is less than 7,000 over the design life (20 years), and so the service is considered static. Under these conditions, $A_3 = 1$.

The factored qualified pressure is equal to the non-factored qualified pressure and, therefore, the qualified stress, σ_{fs}, is determined as follows:

$$\sigma_{fs} = \frac{p_{qf}\ D}{2\,t} = \frac{p_q\ D}{2\,t} = \frac{14.137 \times 100}{2 \times 1} = 706.85\ MPa \tag{6.46}$$

Finally, f_3 can be accessed from equation (6.36), as follows:

$$f_3 = 1 - \frac{2\,\sigma_{ab}}{r\ f_2\ \sigma_{fs}} = 1 - \frac{2 \times 5}{0.185 \times 0.67 \times 706.85} \approx 0.886 \tag{6.47}$$

and pressure rating, p_{NPR}, to be provided in the product literature is determined as:

$$p_{NPR} = f_2\ f_3\ p_q = 0.67 \times 0.886 \times 14.137 = 8.39\ MPa = 83.9\ bar \tag{6.48}$$

The typical nominal pressure rating of this specific GRE pipe ($D = 100\ mm$, $t = 1\ mm$, $\varphi = \pm 55°$) would thus be $PN = 80\ bar$.

In order to establish the long-term failure envelope for this specific GRE pipe, which defines its domain of allowable operating conditions under combined biaxial stress states, one must first determine the idealized long-term failure envelope. This envelope is geometrically identical to the short-term envelope (experimental data in Table 6.5), with the three main data points scaled through f_{scale}, which is given by:

$$f_{scale} = \frac{\sigma_{qs}}{\sigma_{sh(2:1)}} = \frac{\sigma_{fs}}{\sigma_{sh(2:1)}} = \frac{706.85}{736} \approx 0.96 \tag{6.49}$$

Then, the non-factored long-term design envelope is based on this idealized long-term envelope multiplied by f_2. In this particular case, the factored long-term design envelope would be equal to the non-factored design envelope, since all the partial factors (A_1, A_2 and A_3) are equal to unity.

In Figure 6.27 the short-term and long-term envelopes are depicted, based on the short-term experimental data [36] and the factors just calculated above.

6.7 CONCLUSIONS

The aim of the present chapter was to provide a broad description of the present state-of-the-art concerning qualification and preliminary long-term design of filament-wound pipes. The worked examples were mainly focused on angle-ply stacking sequences, especially on the ±55° winding angle. Unfortunately, there is a lack of published experimental data reporting long-term creep failure on filament-wound pipes. Moreover, since qualification standards only mandate one to register the time or cycles to failure, experimental data on creep strain of filament-wound pipes is even scarcer. For obvious reasons, companies are reluctant to publicize important information derived from millions of creep and fatigue testing

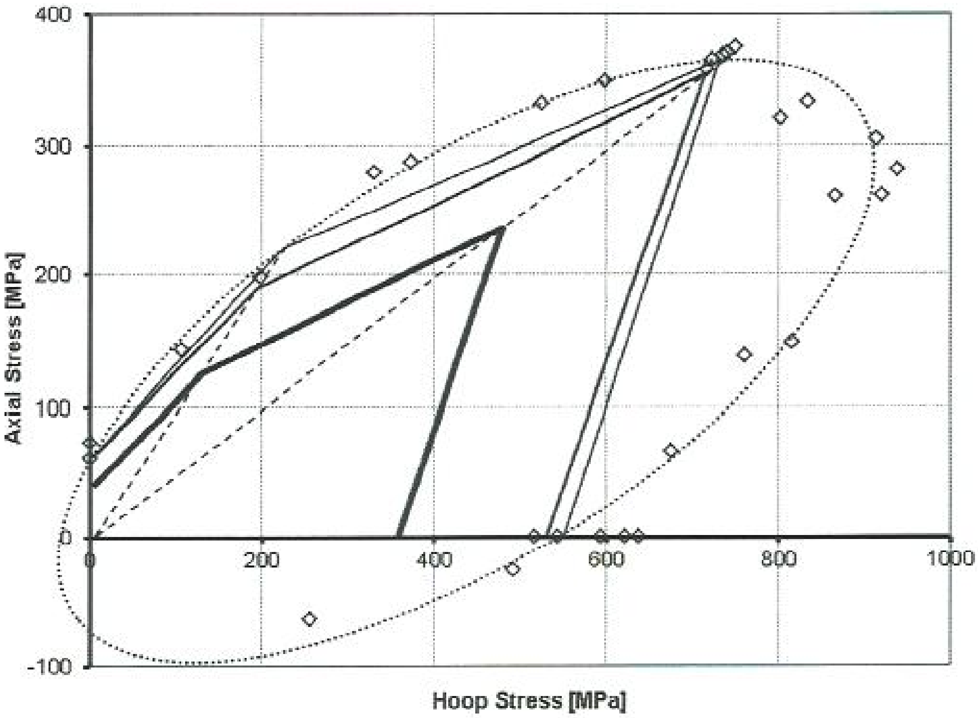

Figure 6.27 Failure envelopes for the selected/designed GRE pipe, calculated in accordance with ISO 14692. Dots are the short-term experimental data. The solid lines represent idealized short-term (thinnest lines), idealized long-term (medium lines) and design long-term (thickest lines) failure envelopes.

hours. Yet fatigue curves for various filament-wound pipes, available in the technical literature, are more substantial. It should be pointed out that damage under cyclic loading is more severe than damage under sustained loading. The standards used for design and qualification of filament-wound pipes, which cover different types of applications, were presented and compared. In the specific case of pipes for oil and gas transportation, one worldwide standard accepted by industry is ISO 14692. The present chapter closed with a worked example based on ISO 14692, which discussed the safety factors used in durability design.

6.8 ACKNOWLEDGEMENTS

Some test series presented here were conducted within research supported by the Growth Programme of the European Commission and the Portuguese Foundation for Science and Technology through projects G6RD-CT2000-00259 and POCTI/EME/47734/2002, respectively. The authors also acknowledge Dr. Catherine Hervé (CETIM) for the data compilation of hydrostatic pressure tests from project G6RD-CT2000-00259 partners.

REFERENCES

[1] Ochoa Ozden O., Salama Mamdouh M. "Offshore composites: Transition barriers to an enabling technology," *Composites Science and Technology* 65:2588–2596, 2005.

[2] Schapery, R. A., (1969), "On the Characterization of Nonlinear Viscolelastic Materials," *Polymer Engineering and Science* 9(4):295–310, 1969.

[3] Ghorbel I., "Durability of closed-end pressurized GRP filament-wound pipes under hygrothermal aging conditions. Part II: creep tests." *Journal of Composite Materials* 30(14): 1581–1595, 1996.

[4] Scott David W., Lai James S. and Zureick Abdul-Hamid. "Creep Behavior of Fiber-Reinforced Polymeric Composites: A Review of the Technical Literature. "*Journal of Reinforced Plastics and Composites* 14: 588–617, 1995.

[5] Guedes R. M. "An energy criterion to predict delayed failure of multi-directional polymer matrix composites based on a non-linear viscoelastic model," *Composites Part A* 35(5): 559–571, 2004.

[6] Guedes R.M. "Nonlinear viscoelastic analysis of thick-walled cylindrical composite pipes." *International Journal of Mechanical Sciences* 52 (8):1064–1073, 2010.

[7] Reiner M., Weissenberg K. "A thermodynamic theory of the strength of the materials." *Rheol Leaflet* 10:12–20, 1939.

[8] Hunter S. C. "Tentative Equations for the Propagation of Stress, Strain and Temperature Fields in Viscoelastic Solids," *J Mech Phys Solids* 9(1):39–51, 1961.

[9] Guedes R.M. "Mathematical analysis of energies for viscoelastic materials and energy based failure criteria for creep loading." *Mechanics of Time-Dependent Materials* 8(2):169–192, 2004.

[10] Guedes RM. "Lifetime predictions of polymer matrix composites under constant or monotonic load." *Composites Part A* 37 (5): 703–715, 2006.

[11] Schapery R. A. "Theory of crack initiation and growth in viscoelastic media. 3. Analysis of continuous growth." *Internat. J. Fracture* 11(4):549–562, 1975.

[12] Christensen R. M. "Lifetime predictions for polymers and composites under constant load." *J. Rheology* 25:517–528, 1981.

[13] Song M.S., Hua G.X. and Hub L.J., "Prediction of long-term mechanical behaviour and lifetime of polymeric materials." *Polymer Testing* 17:311–332, 1998.

[14] Raghavan J., Meshii M. "Creep Rupture of Polymer Composites." *Composite Science and Technology* 57:375–388, 1997.

[15] Zhurkov S.N. "Kinetic concept of the strength of solids." *Int J Fract Mech* 1(4):311–323, 1965.

[16] Griffith W. I. Morris D.H. and Brinson H.F. "The accelerated characterization of viscoelastic composite materials." *Virginia Polytechnic Institute Report VPI-E-80-15*: Blacksburg, VA, 1980.

[17] Knauss W.G. "Delayed failure-the Griffith problem for linearly viscoelastic materials." *Internat. J. Fracture* 6:7–20, 1970.

[18] Kostrov B.V. and Nikitin L.V. "Some general problems of mechanics of brittle fracture." *Arch. Mech. Stos.* (English version) 22:749–776, 1970.

[19] Schapery R.A. "Theory of crack initiation and growth in viscoelastic media. 1. Theoretical development." *Int J Fract* 11(1):141–59, 1975.

[20] Schapery R.A. "Theory of crack initiation and growth in viscoelastic media. 2. Approximate methods of analysis." *Int J Fract* 11(3):369–88, 1975.

[21] Leon R., Weitsman YJ. "Time-to-failure of randomly reinforced glass strand/urethane matrix composites: data, statistical analysis and theoretical prediction." *Mechanics of Materials* 33(3):127–137, 2001.

[22] Ren W. "Creep behavior of a continuous strand, swirl mat reinforced polymeric composite in simulated automotive environments for durability investigation; Part I: experimental development and creep-rupture," *Materials Science and Engineering A* 334(1–2):312–319, 2002.

[23] Christensen R.M., "An evaluation of linear cumulative damage (Miner's Law) using kinetic crack growth theory." *Mech Time-Dependent Mater* 6(4):363–77, 2002.

[24] Kachanov, L. M., "On the Time to Failure Under Creep Conditions." *Izv. Akad. Nauk SSR*, Otd. Tekhn. Nauk 8:26–31, 1958.

[25] Stigh U. "Continuum Damage Mechanics and the Life-Fraction Rule." *Journal of Applied Mechanics* 73(4):702–704, 2006.

[26] Miner M.A. "Cumulative damage in fatigue." *J. Appl. Mech.* 12:A159–A164, 1945.

[27] Bowman J., Barker M.B.A. "Methodology for describing creep–fatigue interactions in thermoplastic components." *Polym Eng Sci* 26(22):1582–90, 1986.

[28] Reifsnider K.L., Stinchcomb W.W. "A critical element model of the residual strength and life of fatigue-loaded composite coupons." In: Hahn HT, editor. *Composite materials: fatigue and fracture (ASTM STP 907)*. Philadelphia (PA): American Society for Testing and Materials; p. 298–313, 1986.

[29] Reifsnider K., Case S., Duthoi J. "The mechanics of composite strength evolution." *Composite Sci Technol* 60:2539–46, 2000.

[30] Reifsnider K., Case S. *Damage tolerance and durability in material systems*. Wiley-Interscience; 2002.

[31] Frost S.R. "Ageing of composite in oil and gas applications," in *Ageing of composites* Edited by R Martin, Woodhead Publishing Limited, Cambridge, 2008.

[32] Roberts S.J., Evans J.T., Gibson A.G., Frost S.R. "The effect of matrix microcracks on the stress-strain relationship in fiber composite tubes." *Journal of Composite Materials* 37 (17):1509–1523, 2003.

[33] Zang W. and Gudmundson P. "An Analytical Model for the Thermoelastic Properties of Composite Laminates Containing Transverse Matrix Cracks," *International Journal of Solids and Structures*, 30: 3211–3231, 1993.

[34] Gudmundson Peter and Östlund Sören."Numerical Verification of a Procedure for Calculation of Elastic Constants in Microcracking Composite Laminates." *Journal of Composite Materials* 26(17):2480–2492, 1992.

[35] Soden P. D., Hinton M. J. and Kaddour A. S. "Lamina properties, lay-up configurations and loading conditions for a range of fibre-reinforced composite laminates." *Composites Science and Technology* 58 (1998) 1011–1022.

[36] Soden P.D., Hinton M.J., Kaddour A.S. "Biaxial test results for strength and deformation of a range of E-glass and carbon fibre reinforced composite laminates: failure exercise benchmark data." *Composites Science and Technology* 62:1489–1514, 2002.

[37] Gibson A.G., Abdul Majid M.S., Assaleh T.A., Hale J.M., Fahrer A., Rookus C.A.P., Hekman M. "Qualification and lifetime modelling of fibreglass pipe." *Plastics, Rubber and Composites* 40 (2):80–85, 2011.

[38] Hale J.M., Gibson A.G., Speake S.D. "Biaxial failure envelope and creep testing of fibre reinforced plastic pipes in high temperature aqueous environments." *Journal of Composite Materials* 36 (3):257–270, 2002.

[39] Soden P.D., Kaddour A.S., Hinton M.J. "Recommendations for designers and researchers resulting from the world-wide failure exercise." *Composites Science and Technology* 64 (3–4):589–604, 2004.

[40] Mieras H.J.M.A. "Irreversible creep of filament-wound glass-reinforced resin pipes," *Plastics & Polymers* 41:84–88, 1973.

[41] Jones M. L. C., Hull D. "Microscopy of failure mechanisms in filament-wound pipe." *Journal of Materials Science* 14:165–174, 1979.

[42] Hull D., Legg M.J., Spencer B. "Failure of glass/polyester filament wound pipe," *Composites 9* (1):17–24, 1978.

[43] Frost S. R. and Cervenka A. "Glass fiber-reinforced epoxy matrix filament-wound pipes for use in the oil industry." *Compos. Manuf.* 5 (2):73–81, 1994.

[44] Gibson A.G., Dodds N., Frost S.R., Sheldrake T. "Novel approach to qualification of non-metallic pipe systems - As applied to reinforced thermoplastic pipe." *Plastics, Rubber and Composites*, 34 (7):301–304, 2005.

[45] Abdul Majid M.S., Assaleh T.A., Gibson A.G., Hale J.M., Fahrer A., Rookus C.A.P., Hekman M. "Ultimate elastic wall stress (UEWS) test of glass fibre reinforced epoxy (GRE) pipe." *Composites: Part A* 42:1500–1508, 2011.

[46] Ghorbel D. Valentin, Yrieix M.-C., Spiteri P. "The effect of resin flexibility on the creep behaviour of filament-wound glass-reinforced resin pipes." *Developments in the science and technology of composite materials: Fourth European Conference on Composite Materials (ECCM4)*, September 25–28, 1990, Stuttgart, F.R.G. J. Füller, European Economic Community.

[47] Faria H., Guedes R.M. "Long-term behaviour of GFRP pipes: Reducing the prediction test duration." *Polymer Testing* 29 (3):337–345, 2010.

[48] Guedes R.M., Sá A., Faria H. "On the prediction of long-term creep-failure of GRP pipes in aqueous environment," *Polymer Composites* 31 (6):1047–1055, 2010.

[49] Gdoutos E. E., Pilakoutas K., Rodopoulos C. A. *Failure analysis of industrial composite materials.* McGraw-Hill Professional; first edition, 2000.

[50] Eckold G., "Mechanics of materials behaviour," Chapter 3 in *Design and Manufacture of Composite Structures*, Woodhead Publishing, Cambridge, 1994 pages 86–88. ISBN 1-85573-051-0.

[51] Evans J.T. and Gibson A.G. "Composite angle ply laminates and netting analysis." *Proceedings of the Royal Society, Part A: Mathematical, Physical and Engineering Sciences* 458:3079-3088, 2002.

[52] Verchery G. "Design of laminates for in-plane loading." *ICCM International Conferences on Composite Materials*, 2009.

[53] Tew B.W. "Preliminary design of tubular composite structures using netting theory and composite degradation factors." *Journal of Pressure Vessel Technology*, Transactions of the ASME 117 (4):390–394, 1995.

[54] *ISO 14692:2002—Petroleum and natural gas industries Glass reinforced plastics (GRP) piping*, International Organization for Standardization, Geneva, 2002.

[55] AWWA M45:2005—*Fiberglass Pipe Design*, 2nd edition, American Water Works Association, Denver, 2005.

[56] Laney Patrick. *Use of Composite Pipe Materials in the Transportation of Natural Gas*, Idaho National Engineering and Environmental Laboratory, Idaho, 2002.

[57] *HOBAS CC-GRP Pipes—Features, Tests and Benefits*, Hobas Engineering GmbH, Klagenfurt, 2010.

[58] *ISO 10928:2009 Plastics piping systems—Glass-reinforced thermosetting plastics (GRP) pipes and fittings—Methods for regression analysis and their use*, International Organization for Standardization, Geneva, 2009.

[59] *EN 1447:2009 Plastics piping systems Glass reinforced thermosetting plastics (GRP) pipes Determination of long term resistance to internal pressure*, European Committee for Standardization, Brussels, 2009.